Journal Pre-proofs

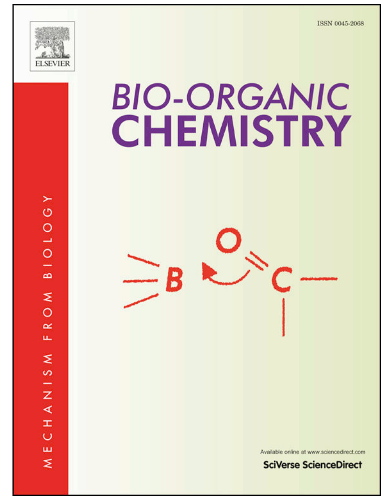

Design, synthesis and pharmacological evaluation of tricyclic derivatives as selective RXFP4 agonists

Lin Lin, Guangyao Lin, Qingtong Zhou, Ross A.D. Bathgate, Grace Qun Gong, Dehua Yang, Qing Liu, Ming-Wei Wang

PII:	S0045-2068(21)00159-0
DOI:	https://doi.org/10.1016/j.bioorg.2021.104782
Reference:	YBIOO 104782

To appear in: *Bioorganic Chemistry*

Received Date:	29 November 2020
Revised Date:	7 February 2021
Accepted Date:	23 February 2021

Please cite this article as: L. Lin, G. Lin, Q. Zhou, R.A.D. Bathgate, G. Qun Gong, D. Yang, Q. Liu, M-W. Wang, Design, synthesis and pharmacological evaluation of tricyclic derivatives as selective RXFP4 agonists, *Bioorganic Chemistry* (2021), doi: https://doi.org/10.1016/j.bioorg.2021.104782

Design, synthesis and pharmacological evaluation of tricyclic derivatives as selective RXFP4 agonists

Lin Lin[a], Guangyao Lin[b,c], Qingtong Zhou[d], Ross A.D. Bathgate[e], Grace Qun Gong[f], Dehua Yang[c,f,*], Qing Liu[f,*] and Ming-Wei Wang[a,b,d,f,*]

[a] *School of Pharmacy, Fudan University, Shanghai 201203, China*

[b] *School of Life Science and Technology, ShanghaiTech University, Shanghai 201210, China*

[c] *University of Chinese Academy of Sciences, Beijing 100049, China*

[d] *School of Basic Medical Sciences, Fudan University, Shanghai 200032, China*

[e] *Florey Institute of Neuroscience and Mental Health, Department of Biochemistry and Molecular Biology, The University of Melbourne, Parkville, VIC 3052, Australia*

[f] *The National Center for Drug Screening and CAS Key Laboratory of Receptor Research, Shanghai Institute of Materia Medica, Chinese Academy of Sciences (CAS), Shanghai 201203, China*

*Correspondence: Ming-Wei Wang (mwwang@simm.ac.cn), Qing Liu (qliu@simm.ac.cn) or Dehua Yang (dhyang@simm.ac.cn).

ABSTRACT

Relaxin family peptide receptors (RXFPs) are the potential therapeutic targets for neuroscience, cardiovascular, and metabolic indications. Among them, RXFP3 and RXFP4 (formerly known as GPR100 or GPCR142) are homologous class A G protein-coupled receptors with short N-terminal domain. Ligands of RXFP3 or RXFP4 are only limited to endogenous peptides and their analogues, and no natural product or synthetic agonists have been reported to date except for a scaffold of indole-containing derivatives as dual agonists of RXFP3 and RXFP4. In this study, a new scaffold of tricyclic derivatives represented by compound **7a** was disclosed as a selective RXFP4 agonist after a high-throughput screening campaign against a diverse library of 52,000 synthetic and natural compounds. Two rounds of structural modification around this scaffold were performed focusing on three parts: 2-chlorophenyl group, 4-hydroxylphenyl group and its skeleton including cyclohexane-1,3-dione and 1,2,4-triazole group. Compound **14b** with a new skeleton of 7,9-dihydro-4*H*-thiopyrano[3,4-d][1,2,4]triazolo[1,5-a]pyrimidin-8(5*H*)-one was thus obtained. The enantiomers of **7a** and **14b** were also resolved with their 9-(*S*)-conformer favoring RXFP4 agonism.

Compared with **7a**, compound 9-(*S*)-**14b** exhibited 2.3-fold higher efficacy and better selectivity for RXFP4 (selective ratio of RXFP4 *vs.* RXFP3 for 9-(*S*)-**14b** and **7a** were 26.9 and 13.9, respectively).

Graphical abstract

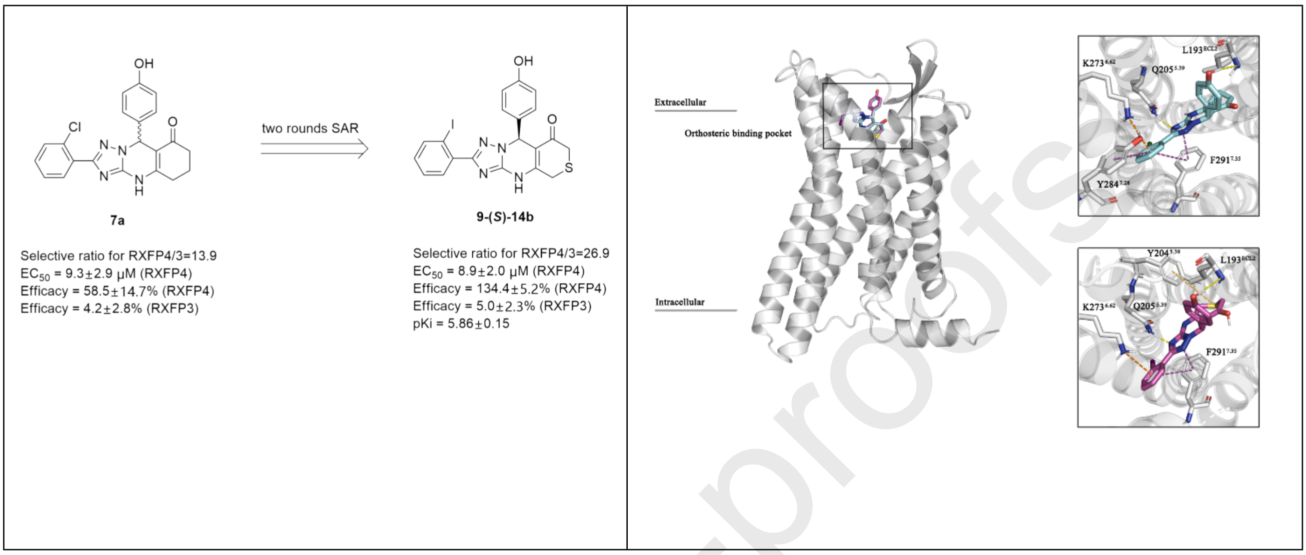

KEYWORDS

Synthesis, structure-activity relationship, relaxin family peptide receptor 4, selective agonist, molecular docking.

Glossary

HTRF	Homogeneous time-resolved fluorescence
HTS	High-throughput screening
SAR	Structure-activity relationship
RXFPs1-4	Relaxin family peptide receptors 1-4
GPCRs	G protein-coupled receptors

Highlights

A series of tricyclic derivatives were synthesized *via* Biginelli cyclocondensation.

The analogues were screened for their biological activities using a HTRF assay that measures the inhibition of forskolin-stimulated cAMP accumulation in human RXFP4-overexpressing CHO cells.

The specificity of the analogues for RXFP4 was also examined in human RXFP3-overexpressing CHO-K1 cells and human RXFP1-overexpressing 293T cells.

Compared with **7a**, compound 9-(*S*)-**14b** behaved as a RXFP4 agonist and exhibited 2.3-fold higher efficacy and better selectivity for RXFP4 *vs.* RXFP3.

A relatively high LibDock fitness score of 111.977 was obtained for the docking of **14b** with RXFP4, and several functions were involved including two hydrogen bonds, Pi-Pi stack and Pi-cation individually, and one additional Pi-sulfur function, which may explain the efficacy difference between **14b** and **7a**.

1. Introduction

Relaxin family is a group of peptide hormones that perform a variety of biological functions after activation of the relaxin family peptide receptors 1-4 (RXFPs1-4) [1,2], such as reproduction regulation, stress responses, food intake and glucose homeostasis, *etc.* These associated activities enable RXFPs to be the potential therapeutic targets for neurological, cardiovascular and metabolic disorders [3-9]. Among them, RXFP3 and RXFP4 (formerly known as GPR100 or GPCR142) are homologous class A G protein-coupled receptors (GPCRs) with a short N-terminal domain. RXFP4 is predominantly expressed in the colon and rectum with implications of insulin secretion, appetite and regulation of colon motility [1,10]. The cognate ligands of RXFP3 and RXFP4 are relaxin-3 and insulin-like peptide 5 (INSL5), respectively. Relaxin-3 also activates RXFP1 and RXFP4 *in vitro* [8,11]. Relaxin-3 interacts with both the LRR domain and ECL2 of the TM domain of RXFP1 to produce the full binding and cAMP signaling profile [2]. R3/I5, a chimeric peptide, contains the B chain of relaxin-3 and the A chain of INSL5 and activates RXFP3 and RXFP4 at almost equal potency [2]. INSL5 is a two-chain, three-disulfide-bonded peptide and mainly expressed in the colorectum and enteric nervous system together with glucagon-like peptide 1 (GLP-1) and peptide YY. Binding of INSL5 to RXFP4 increases GTPγS activity, inhibits forskolin-stimulated cyclic adenosine monophosphate (cAMP) accumulation and elevates phosphorylation of ERK1/2, p38MAPK, Akt Ser^{473}, Akt Thr^{308} and S6 ribosomal protein in CHO-RXFP4 cells [1,12]. INSL5 also suppresses glucose-stimulated insulin secretion and Ca^{2+} mobilization in MIN6 insulinoma cells and forskolin-stimulated cAMP accumulation in NCI-H716 enteroendocrine cells [12]. Despite these attractive properties, ligands of RXFP3 or RXFP4 are only limited to endogenous peptides and their analogues, and no natural product or synthetic agonists have been reported to date except for a scaffold of indole-containing derivatives disclosed by DeChristopher and colleagues as dual agonists of RXFP3 and RXFP4 (shown as compound **1** in Figure 1) [13].

In an attempt to discover non-peptidic small molecules as selective RXFP4 agonists, a high-throughput screening (HTS) campaign against a diverse library of 52,000 synthetic and natural compounds was carried out using a homogeneous time-resolved fluorescence (HTRF) assay that measures the inhibition of forskolin-stimulated cAMP accumulation in human RXFP3- and RXFP4-overexpressing CHO cells. This led to the discovery of a new scaffold, 5,6,7,9-tetrahydro-[1,2,4]triazolo[5,1-b]quinazolin-8(4*H*)-one (represented by **7a**), as selective RXFP4 agonist as demonstrated by its activities in pCRE activation, ERK1/2 phosphorylation, intracellular calcium mobilization and β-arrestin recruitment [14]. In this paper, we described in detail their chemical synthesis, structure-activity relationship (SAR) analysis, molecular docking and subsequent bioactivity evaluation.

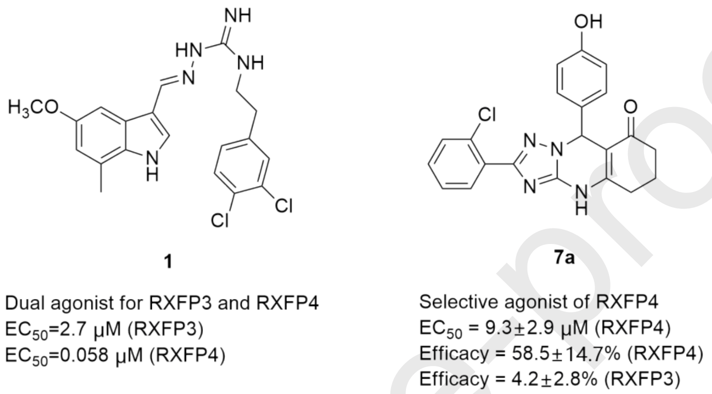

Figure 1. Structures of compounds 1 and 7a.

2. Results and Discussion

2.1. SAR-based design and chemical synthesis

Based on SAR information, rational design around the scaffold of 5,6,7,9-tetrahydro-[1,2,4]triazolo[5,1-b]quinazolin-8(4*H*)-one (represented by **7a**) was conducted focusing on five parts: 2-chlorophenyl group, 4-hydroxylphenyl group, its skeleton including cyclohexane-1,3-dione and 1,2,4-triazole group, and chiral resolution (Figure 2).

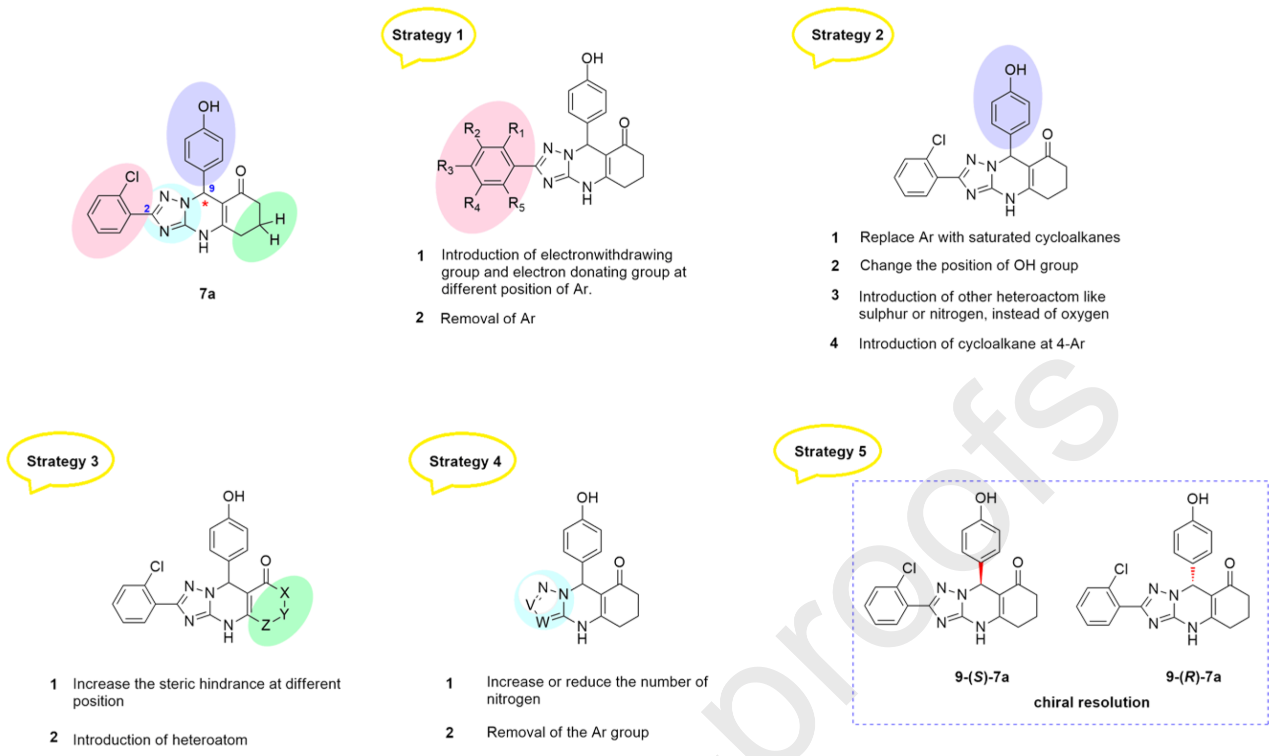

Figure 2. Rational design of RXFP4 agonists.

The general synthetic route is described as follows. Substituted methyl benzoate **2** or benzoyl chloride **3** was used as the starting material, which underwent hydrazinolysis to obtain benzohydrazide derivatives **4.** The key intermediate 1,2,4-triazole **6** was synthesized by reacting compound **4** with *S*-methylisothiourea sulfate which was cyclized in the following step using *p*-toluenesulfonic acid as a catalyst. Biginelli cyclocondensation [15-17] was then conducted under the catalysis of acetic acid with the triazole derivative **6**, cyclohexane-1,3-dione and 4-hydroxybenzaldehyde to obtain the final product **7** (Scheme 1). Compound **7a-m** were then designed and synthesized for the purpose of finding the suitable substitutes on the phenyl group by involving the electron-donating group (**7h-i**), electron-withdrawing group (**7a-g** and **7j-l**), the effect of steric-hindrance (**7f-g**) or the substituted position (**7a-c** and **7j-l**) to improve their binding to RXFP4.

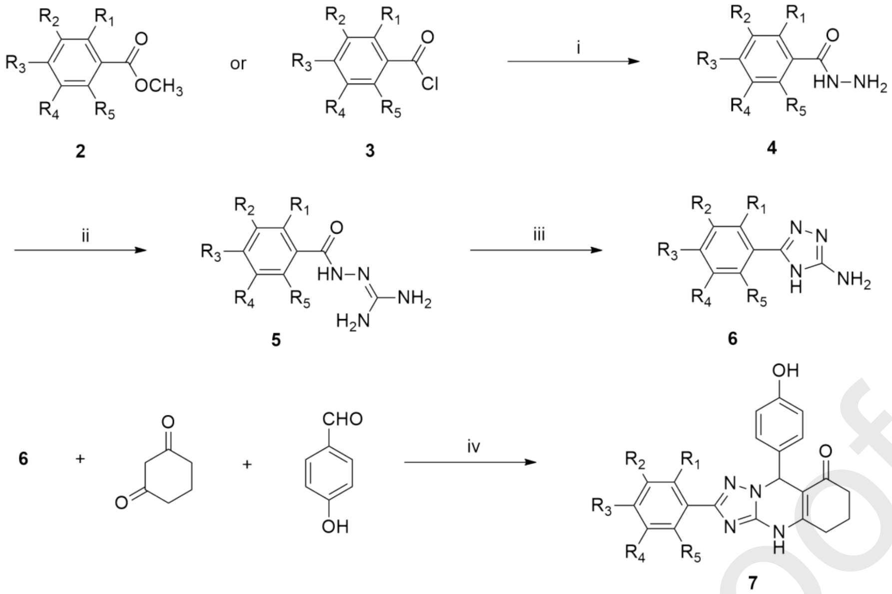

2-7 a	R_1 = Cl, $R_2 = R_3 = R_4 = R_5$ = H	**2-7 h**	R_2 = OMe, $R_1 = R_3 = R_4 = R_5$ = H
2-7 b	R_2 = Cl, $R_1 = R_3 = R_4 = R_5$ = H	**2-7 i**	R_3 = OMe, $R_2 = R_1 = R_4 = R_5$ = H
2-7 c	R_3 = Cl, $R_2 = R_1 = R_4 = R_5$ = H	**2-7 j**	$R_1 = R_2$ = Cl, $R_3 = R_4 = R_5$ = H
2-7 d	R_1 = F, $R_2 = R_3 = R_4 = R_5$ = H	**2-7 k**	$R_1 = R_3$ = Cl, $R_2 = R_4 = R_5$ = H
2-7 e	R_1 = Br, $R_2 = R_3 = R_4 = R_5$ = H	**2-7 l**	$R_1 = R_4$ = Cl, $R_2 = R_3 = R_5$ = H
2-7 f	R_1 = I, $R_2 = R_3 = R_4 = R_5$ = H	**2-7 m**	$R_1 = R_2 = R_3 = R_4 = R_5$ = H
2-7 g	$R_1 = CF_3$, $R_2 = R_3 = R_4 = R_5$ = H		

Scheme 1. Synthetic route for compounds **7a-m**. (i) **2** and $NH_2NH_2·H_2O$ in EtOH, reflux or **3** and $NH_2NH_2·H_2O$ in DCM, r.t. overnight; (ii) **4** and *S*-methylisothiourea sulfate in dioxane and 2N NaOH, reflux, two steps yield: 70-98%; (iii) **5** and *p*-TsOH in water and dioxane, reflux, yield: 75-97%; (iv) HOAc in EtOH, reflux, yield: 30-61%.

Subsequent SAR studies around 4-hydroxylphenyl and cyclohexane-1,3-dione were carried out using a similar procedure**,** except that different substituted benzaldehyde **8** and 1,3-cycloalkandione **10** were employed to obtain derivatives **9** and **11**, respectively. Compounds **9a-i** were thus designed and synthesized for the purpose of examining the necessity of 9-aromatic nucleus (**9b**), restriction of the number and position for 4-hydroxyl group (**9a** and **9c**), effect of steric hindrance (**9d** and **9h**) and possibility of introduction of other heteroatom instead of oxygen (**9d-e** and **9g-i**). Compounds **11a-d** were synthesized for the purpose of increasing the steric hindrance (**11a-b**) by addition of di-methyl group and inserting heteroatom such as oxygen (**11c**) and sulphur (**11d**), aiming at finding other possible scaffolds except for 5,6,7,9-tetrahydro-[1,2,4]triazolo[5,1-b]quinazolin-8(4*H*)-one, *e.g.*, compounds **7** and **9**.

Further SAR analysis was made around the skeleton of 1,2,4-triazole part with 4*H*-1,2,4-triazol-3-amine (**12a**) and tetrazole (**12b**) instead of 5-(2-chlorophenyl)-4*H*-1,2,4-triazol-3-amine **6a** to examine if the 2-chlorophenyl group is required for RXFP4 binding. Compounds **13a** and **13b** were thus synthesized. Additionally, a derivative **13c** was synthesized with only two nitrogen atoms involved as compared with compound **7a** to see whether the number of nitrogen atom has any impact on its bioactivity (Scheme 2).

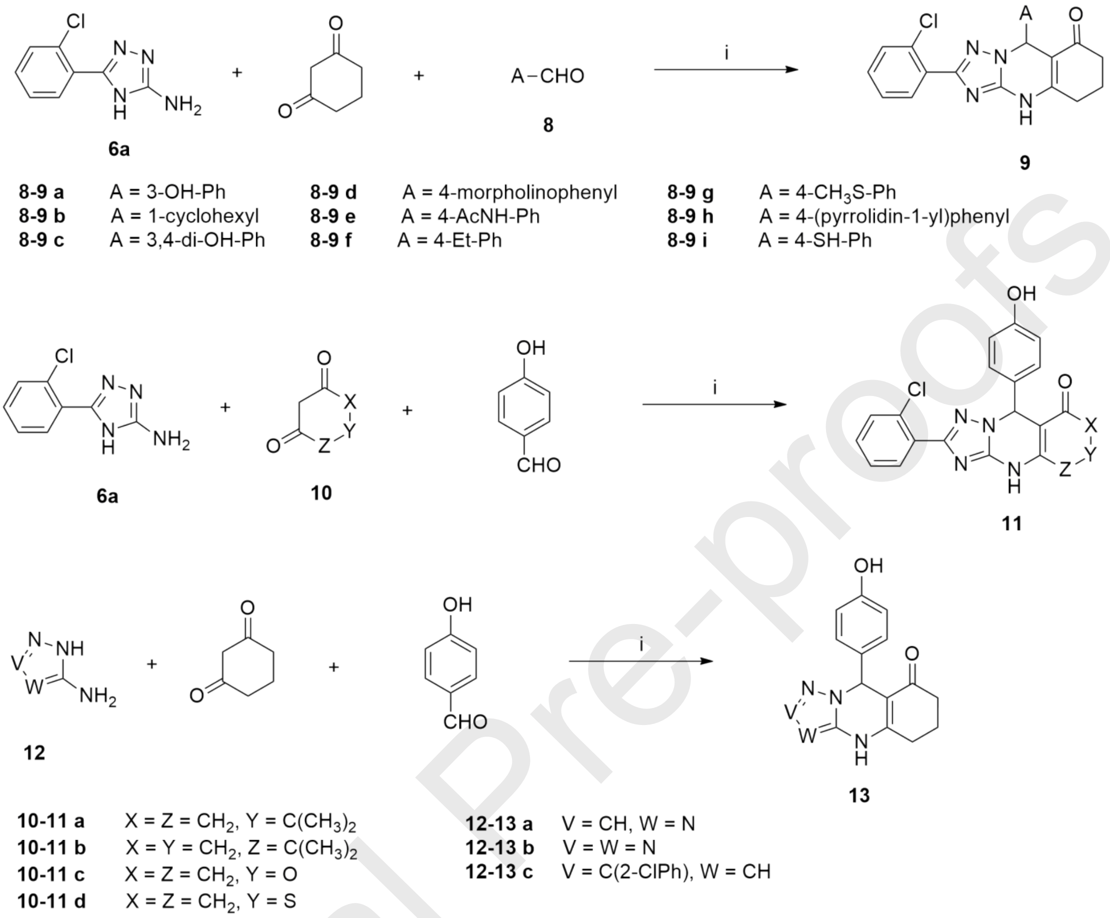

Scheme 2. Synthetic route for compounds **9a-i**, **11a-d** and **13a-c**. (i) HOAc in EtOH, reflux, yields for **9**: 36-59%; **11**: 57-67%; **13**: 69-76%.

2.2. Chiral resolution

The enantiomers of compound **7a** were resolved by CHIRALPAKIC (IC00CD-NA012) column (0.46 cm × 15 cm) on Shimadzu LC-20AT HPLC eluting with dichloromethane/ethanol = 90/10 (*v*/*v*) at a flow rate of 1.0 mL/min (35°C). Two peaks were separately collected at *tR* = 2.090 min (isomer 1) and *tR* = 2.409 min (isomer 2) and the enantiomeric excess (*e.e.*) value of each product was above 98% (Figure 3A). The white block-shaped single crystal of isomer 1 was acquired with orthorhombic crystal system and its X-ray diffraction data were collected on a Bruker D8 VENTURE single-crystal diffractometer. The absolute configuration of isomer 1 was determined as 9-(*R*)-**7a**. Its molecular structure was made up of one aromatic heterocycle, two aromatic rings and one aliphatic ring. The 2-chlorophenyl ring was almost coplanar with the middle tricycle (Figure 3B). The crystallographic data was shown in Table S1-

6 (Supplementary Information). CCDC2004638 contains the supplementary crystallographic data for compound 9-(*R*)-**7a** and could be obtained free of charge from The Cambridge Crystallographic Data Centre *via* www.ccdc.cam.ac.uk/data_request/cif.

A

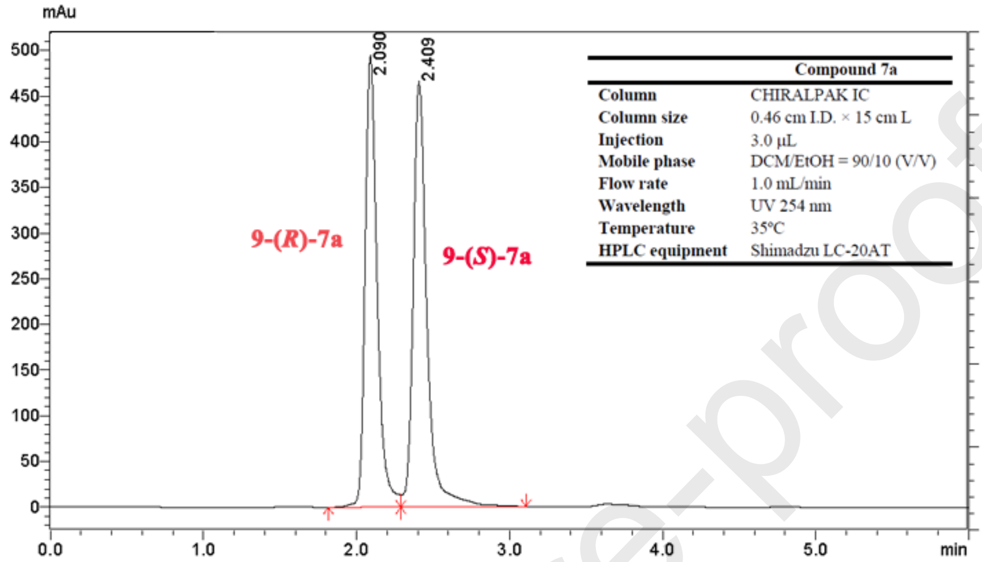

B

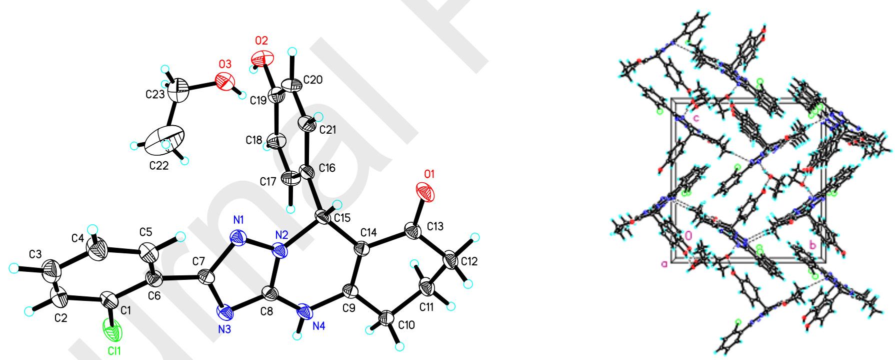

Figure 3. Chiral resolution of compound 7a. **A**, The condition of chiral resolution and its chromatography; **B**, Crystal structure of 9-(*R*)-**7a** with the atom labelling.

2.3. cAMP accumulation and SAR analysis

RXFP4 agonist activities of compounds **7**, **9**, **11** and **13** were evaluated with a homogeneous time-resolved fluorescence (HTRF) assay that measures the inhibition of forskolin-stimulated cAMP accumulation in human RXFP4-overexpressing CHO cells. The specificity of these compounds for RXFP4 was also examined in CHO-K1 cells stably expressing the human RXFP3, which is the most closely related receptor to RXFP4, and RXFP1, which could be activated by the same endogenous peptide relaxin-

3. Agonist activity was expressed as % INSL5 in hRXFP4-CHO-K1 cells, % R3/I5 in hRXFP3-CHO-K1 cells or % relaxin-3 in hRXFP1-293T cells (Table 1, Figures S1 and S3).

Compound **7a** was capable of inhibiting cAMP accumulation in hRXFP4 overexpressing CHO-K1 cells, while exhibiting little or no agonist activity in hRXFP3-overexpressing CHO-K1 cells and hRXFP1- overexpressing 293T cells (EC_{50} = 9.3±2.9 μM for RXFP4, Efficacy = 58.5±14.7% for RXFP4 and 4.2±2.8% for RXFP3, respectively), indicating that this agonism was selective (Figures 4A, 4B and S3). Compound **7a** also activated RXFP4-mediated signaling pathways including ERK1/2 phosphorylation and β-arrestin 1/2 recruitment [14]. Chiral resolution of compound **7a** resulted in a couple of enantiomers 9-(*S*)-**7a** and 9-(*R*)-**7a** with its 9-(*S*)-conformer displaying full agonism as INSL5 (Efficacy = 106.6±9.9% and 22.3±9.3% for RXFP4 and RXFP3, respectively), while its 9-(*R*)-conformer was inactive in both RXFP4- and RXFP3-overexpressing cells.

A

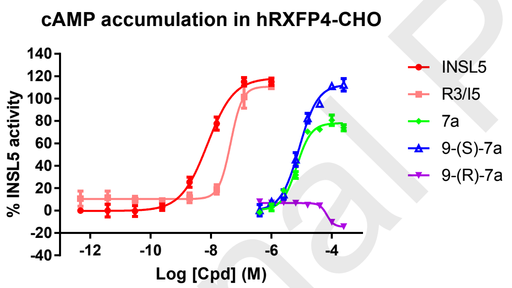

B

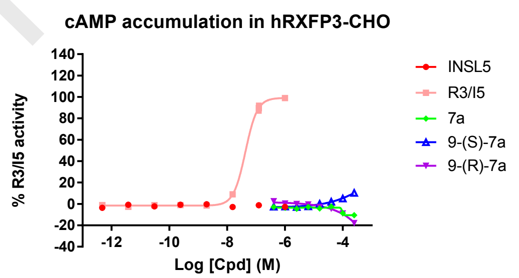

C

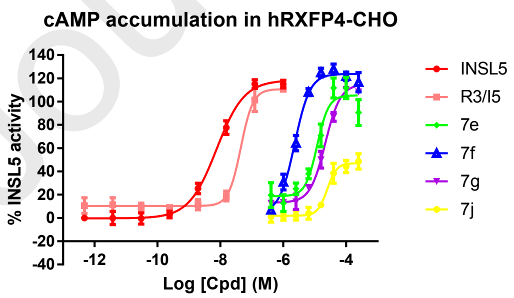

D

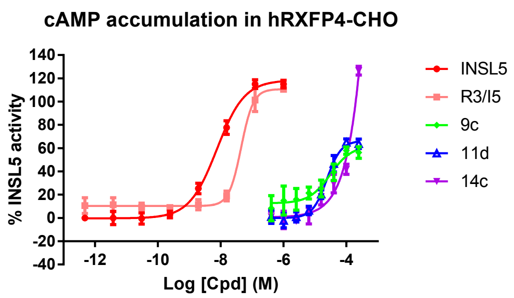

E

F

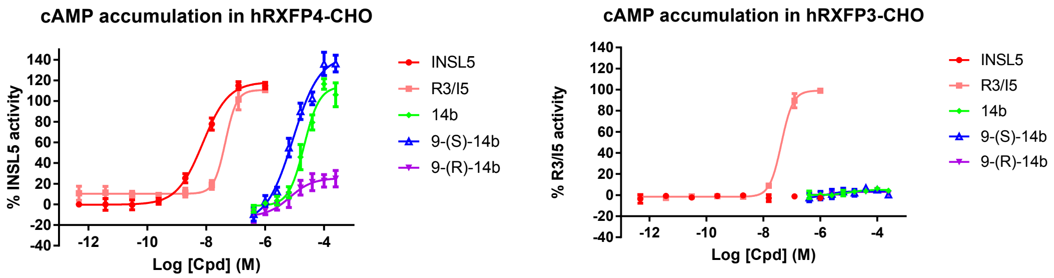

Figure 4. Inhibition of forskolin-stimulated cAMP accumulation by test compounds in CHO-K1 cells overexpressing hRXFP4 or hRXFP3 (A-F). Each compound was tested in duplicate and each experiment was repeated for three times. Agonist activity was expressed as % INSL5 in hRXFP4-CHO-K1 cells or % R3/I5 in hRXFP3-CHO-K1 cells. For each concentration, the value of 665/615 was calculated, and normalized to the corresponding maximum value obtained for INSL5 in hRXFP4-CHO-K1 cells and for R3/I5 in hRXFP3-CHO-K1 cells. Normalized values were plotted *vs*. ligand concentration using GraphPad PRISM 8 and are expressed as means ± SEM. Cpd, compound.

It follows that shifting the position of 2-chloro group (strategy 1 in Figure 2) from *ortho*- to that of *meta*- or *para*- resulted in a total loss of activity (**7a** *vs*. **7b** and **7c**). The size of atomic radius (**7d**: R_1 = F; **7a**: R_1 = Cl; **7e**: R_1 = Br; **7f**: R_1 = I) also affected bioactivity with the tendency that the bigger the atomic radius, the higher the agonist effect, *i.e.*, 2-iodine substituted analogue **7f** showed 96.2±9.1% efficacy of INSL5, while its potency was also elevated by nearly 4.9-fold compared to **7a** (EC_{50}=1.9±0.3 μM for **7f** and EC_{50}=9.3±2.9 μM for **7a**). Similar phenomenon was observed for **7g** (2-CF_3) that has a bigger steric hindrance than **7a** (2-Cl) and exhibited almost an equal efficacy (93.3±11.2%) to **7f**. Dual chloro-substituted analogues, such as 2,3-*di*-Cl (**7j**), 2,4-*di*-Cl (**7k**) and 2,5-*di*-Cl (**7l**) were designed for examining the optimal substituted position of chloro group. The results showed that compounds with 2,3-*di*-Cl (**7j**) or 2,4-*di*-Cl (**7k**) maintained about 63%-78% efficacy while 2,5-*di*-Cl (**7l**) displayed only 1/3 efficacy compared to **7a**. Removal of this 2-chloro group led to nearly 60% decrease in agonist activity (**7m** *vs*. **7a**). The above observations indicate that 2-position on the phenyl group is essential.

The inhibitory effects on forskolin-stimulated cAMP accumulation in compounds with modifications around 4-hydroxyl phenyl part (strategy 2 in Figure 2, **9a-i**) suggest that this part is crucial for selective binding to RXFP4. Change of 4-OH group to 3-OH and 9-aromatic nucleus to cyclohexyl group led to 70% reduction and a total loss of efficacy, respectively (**9a** and **9b** *vs.* **7a**). 3,4-Dihydroxyl substituted derivative (**9c**) only retained 65% efficacy as **9a**. Of note is that increase of steric hindrance such as 4-morpholinophenyl (**9d**) and 4-(pyrrolidin-1-yl)phenyl (**9h**) caused a weak agonist effect on RXFP3 (Efficacy = 18.3±6.2% for **9h**), indicating that 4-phenyl position may be a key site that defines receptor selectivity. Replacement of 4-OH group with 4-SH could maintain its RXFP4 agonistic activity, however, the potency was nearly decreased by 2-fold (**9i** *vs.* **7a**).

Subsequent studies on the cyclohexane-1,3-dione skeleton was performed through inserting a dimethyl group thereby increasing the steric hindrance, *i.e.*, **11a** and **11b** synthesized by Biginelli cyclocondensation of 5,5-dimethylcyclohexane-1,3-dione (**10a**)/4,4-dimethylcyclohexane-1,3-dione (**10b**) with 3-amine-5-(2-chlorophenyl)-4*H*-1,2,4-triazol (**6a**) and 4-hydroxybenzaldehyde. A sharp reduction in agonism was observed (Efficacy = 9.9±1.2% for **11a** and 18.3±3.5% for **11b**, respectively), suggesting that cyclohexane-1,3-dione skeleton is not tolerant to structural modification. Next, we tried to insert heteroatom to the cyclohexane-1,3-dione skeleton, such as oxygen for **11c** and sulphur for **11d**. In comparison with cyclohexane-1,3-dione skeleton (**7a**), 2*H*-thiopyran-3,5(4*H*,6*H*)-dione skeleton (**11d**) still retained the agonist effect while 2*H*-pyran-3,5(4*H*,6*H*)-dione skeleton (**11c**) significantly decreased its agonist activity (Efficacy = 10.5±2.4% for **11c** and 60.8±7.6% for **11d**, respectively).

For the 1,2,4-triazole skeleton, replacing its triazole group (**7a**) with pyrazole (**13c**) and keeping other substitutes unchanged resulted in complete loss of activity. Removal of 2-chlorophenyl from this skeleton (**13a** *vs.* **7a**) or substitution of 1,2,4-triazole with tetrazole (**13b** *vs.* **7a**) caused a marked decline in agonism, indicating that 3-phenyl-1,2,4-triazole skeleton is an important functional group.

Table 1. Inhibition of forskolin-stimulated cAMP accumulation by synthetic compounds in CHO-K1 cells stably overexpressing hRXFP4 or hRXFP3.[a]

Cpd	EC_{50} (μM)[b]		Efficacy (%)[c]		Cpd	EC_{50} (μM)[b]		Efficacy (%)[c]	
	RXFP4	RXFP3	RXFP4	RXFP3		RXFP4	RXFP3	RXFP4	RXFP3
7a	9.3±2.9	N.D.	58.5±14.7	4.2±2.8	**9d**	50.2±10.5	N.D.	33.9±8.1	6.93[e]
9-*R*-7a	N.D.	N.D.	N.A.	N.A.	**9e**	N.D.	N.D.	7.0±1.6	N.A.
9-*S*-7a	6.8±1.3	230.2±148.0	106.6±9.9	22.3±9.3	**9f**	N.D.	N.D.	N.A.	8.2[e]
7b	N.D.	N.D.	N.A.	N.A.	**9g**	N.D.	N.D.	N.A.	10.4[e]
7c	N.D.	N.D.	6.5±0.4	N.A.	**9h**[d]	N.D.	97.2±11.0	N.A	18.3±6.2
7d	11.8±6.2	N.D.	17.6±4.7	N.A.	**9i**	18.7±3.5	N.D.	52.3±12.3	N.A.
7e	7.1±3.4	N.D.	78.2±5.3	5.34[e]	**11a**	19.3±12.3	N.D.	9.9±1.2	N.A.
7f	1.9±0.3	30.7[e]	96.2±9.1	13.6[e]	**11b**	6.5±2.3	N.D.	18.3±3.5	N.A.
7g	26.5±9.6	141.9[e]	93.3±11.2	13.6[e]	**11c**	35.2±12.3	N.D.	10.5±2.4	N.A.

7h	216±41.0	N.D.	30.4±6.0	N.A.	**11d**	21.6±0.9	26.4	60.8±7.6	8.17[e]
7i	N.D.	N.D.	12.4±4.6	N.A.	**13a**	N.D.	N.D.	9.2±1.5	N.A.
7j	40.6±15.1	N.D.	36.9±3.5	N.A.	**13b**	99.8±5.6	N.D.	13.1±7.3	N.A.
7k	N.D.	N.D.	45.7±6.5	2.54[e]	**13c**	N.D.	N.D.	N.A.	N.A.
7l	22.8±14.8	N.D.	21.3±3.4	N.A.	**14a**	6.0±1.1	N.D.	76.0±12.3	N.A.
7m	N.D.	N.D.	24.6±9.2	N.A.	**14b**	13.8±5.4	N.D.	113.9±13.9	6.2±1.2
9a	N.D.	N.D.	17.1±3.2	N.A.	**9-*R*-**	3.9±2.2	N.D.	27.8±8.9	2.7±0.6
9b	N.D.	N.D.	N.A.	N.A.	**9-*S*-**	8.9±2.0	N.D.	134.4±5.2	5.0±2.3
9c	21.8±9.9	N.D.	38.1±9.0	N.A.	**14c**	N.D.	N.D.	>100.0	>100.0
INSL5	0.011±0.0	N.D.	100	N.A.	**R3/I**	0.045±0.0	0.2±0.1	84.5±3.5	100

[a]Each compound was tested in duplicate and each experiment was repeated at least for three times. [b]EC_{50} values are presented as means ± SEM. [c]Agonist activity is expressed as % INSL5 in hRXFP4-CHO-K1 cells or % R3/I5 in hRXFP3-CHO-K1 cells. [d]The HCl salt of compound **9h** was used in the test. [e]Compound was tested only once. Cpd, compound; N.D., not detectable; N.A., not active.

2.4. Physicochemical properties

Physicochemical properties of synthesized compounds were calculated according to both Lipinisk's rule of five and Veber's rule through selecting appropriate molecules based on size, molecular weight (MW), number of hydrogen bond donors (nHBD) and acceptors (nHBA), molecular octanol/water partition coefficient (MolLogP), number of rotatable bonds (nRotB) and molecular polar surface area (MolPSA). This was carried out using Molsoft online software (http://molsoft.com/mprop/) and Molinspiration cheminformatics software (https://www.molinspiration.com/). Other parameters like molecular water solubility (MolLogS), molecular volume (MolVol) and drug-likeness score were also assessed *in silico* (Table 2). A positive compound is determined when (i) nHBD is ≤5; (ii) nHBA is ≤10; (iii) MW is ≤500; (iv) MolLogP is < 5; (v) nRotB is ≤10; and (vi) PSA is ≤140 Å^2 or nHBD + nHBA ≤12. Our analyses revealed that most of these synthesized compounds conform to the two rules, indicative of optimal membrane permeability, sound bioavailability and acceptable druggability (Table 2).

Table 2. Calculated physicochemical properties of synthesized compounds.

Cpd	**MolLogS**	**MolLogP**	**MW**	**nHBD**	**nHBA**	**nSC**	**nRotB**	**MolVol (A^3)**	**MolPSA (A^2)**	**Drug-likeness model score**
7a	-5.69	4.08	392.1	2	4	1	2	372.53	67.96	1.21
7b	-6.05	4.2	392.1	2	4	1	2	374.56	67.96	0.7
7c	-6.07	4.2	392.1	2	4	1	2	374.48	67.96	0.74
7d	-5.73	3.63	376.13	2	4	1	2	362.08	67.96	1.01
7e	-6.00	4.21	436.05	2	4	1	2	378.22	67.96	0.88

7f	-6.20	4.16	484.04	2	4	1	2	385.73	67.96	1.15
7g	-5.91	4.6	426.13	2	4	1	3	394.3	67.96	0.67
7h	-5.30	3.57	388.15	2	5	1	3	389.21	75.51	0.83
7i	-5.37	3.57	388.15	2	5	1	3	389.13	75.51	0.67
7j	-6.60	4.67	426.07	2	4	1	2	388.2	67.96	1.06
7k	-6.62	4.79	426.07	2	4	1	2	389.8	67.96	1.19
7l	-6.56	4.79	426.07	2	4	1	2	389.8	67.96	0.95
7m	-5.11	3.48	358.14	2	4	1	2	357.29	67.96	0.66
9a	-5.71	4.08	392.1	2	4	1	2	372.6	67.96	0.95
9b	-5.70	4.61	382.16	1	3	1	2	393.03	50.54	0.48
9c	-3.89	3.53	408.10	3	5	1	2	385.25	83.44	1.16
9d	-4.71	4.22	461.16	1	4	1	3	447.99	61.71	0.50
9e	-4.41	3.68	433.13	2	4	1	3	422.94	73.61	1.18
9f	-5.67	5.45 (>5)	404.14	1	3	1	3	401.06	50.34	1.18
9g	-5.42	5.13 (> 5)	422.10	1	4	1	3	399.73	50.34	0.94
9h	-5.70	5.31 (> 5)	445.17	1	3	1	3	440.74	54.16	0.72
9i	-5.02	4.81	408.08	2	4	1	2	378.40	50.34	0.95
11a	-7.34	4.8	420.14	2	4	1	2	418.86	67.96	1.03
11b	-6.75	4.86	420.14	2	4	1	2	415.37	68.12	1.43
11c	-5.33	2.77	394.08	2	5	1	2	358.12	76.87	1.01
11d	-6.85	3.08	410.06	2	5	1	2	374.53	67.96	1.07
13a	-3.27	1.46	282.11	2	4	1	1	283.32	69.17	0.74
13b	-3.15	1.34	283.11	2	5	1	1	277.09	83.65	0.41
13c	-5.72	4.11	391.11	2	3	1	2	374.22	57.33	0.86
14a	-3.98	3.88	454.01	2	5	1	2	380.21	67.96	0.50
14b	-4.02	4.10	502.00	2	5	1	2	387.73	67.96	0.80
14c	-4.15	3.97	444.09	2	5	1	3	396.29	67.96	0.36

All the calculations were carried out online. MolLogS, molecular water solubility in Log (moles/L); MolLogP, molecular octanol/water partition coefficient; nHBD, number of hydrogen bond donors; nHBA, number of hydrogen bond acceptors; nSC, number of stereo centers; nRotB, number of rotatable bonds; MolVol, molecular volume; MolPSA, molecular polar surface area. Drug-likeness score predicts an overall drug-likeness (druggability) using Molsoft's chemical fingerprints. The training set for this mode consists of 5,000 known drugs from WDI (positives) and 100,000 carefully selected non-drug-like compounds (negatives).

2.5. Further optimization

Based on the above SAR studies, several conclusions could be drawn: 2-Br, 2-I and 2-

CF_3 substitutes are superior to 2-Cl (**7e**, **7f** and **7g** *vs.* **7a**, strategy 1 in Figure 2); 4-OH phenyl is an essential group for receptor selectivity (strategy 2 in Figure 2); the skeleton of 5,6,7,9-tetrahydro-[1,2,4]triazolo[5,1-b]quinazolin-8(4*H*)-one (**7a**) could be changed to 7,9-dihydro-4H-thiopyrano[3,4-d][1,2,4]triazolo[1,5-a]pyrimidin-8(5*H*)-one (**11d**) without affecting the agonist effect on RXFP4 (strategy 3 in Figure 2); and 3-phenyl-1,2,4-triazole skeleton is an key functional group for RXFP4 binding (strategy 4 in Figure 2). We then conducted the 2nd round structural optimization for the purpose of combining these proponent functional groups. Compounds **14a-c** were thus made by Biginelli cyclocondensation of 5-(2-bromophenyl)-4*H*-1,2,4-triazol-3-amine (**6e**), or 5-(2-iodophenyl)-4*H*-1,2,4-triazol-3-amine (**6f**), or 5-(2-(trifluoromethyl)phenyl)-4*H*-1,2,4-triazol-3-amine (**6g**), cyclohexane-1,3-dione/2*H*-thiopyran-3,5(4*H*, 6*H*)-dione and 4-hydroxybenzaldehyde under the catalysis of acetic acid (Scheme 3). They were subsequently examined with cAMP accumulation assay. Similar phenomenon was observed for strategy 1 (Figure 2) that bigger steric hindrance was beneficial to its RXFP4 agonism as compared with compounds **14a** and **14b** (Efficacy = 76.0±12.3 for **14a** and 113.9±13.9 for **14b**, respectively). Of these three compounds, **14b** exhibited the highest efficacy, close to that of the isomer 9-(*S*)-**7a** with better selective ratio for RXFP4 than RXFP3 (18.4 and 4.8 for **14b** and 9-(*S*)-**7a**, respectively; Table 1). Also, compound **14b** showed no agonistic effect on RXFP1 (Figure S3). In addition, the solubility of **14b** was ameliorated compared to **7a** (MolLog S = -4.02 and -5.69 for **14b** and **7a**, respectively; Table 2). Next, the enantiomers of compound **14b** were resolved by CHIRALPAK IC column (0.46 cm × 15 cm) on Shimadzu LC-2010 HPLC eluting with ethanol with a flow rate of 1.0 mL/min at 25°C. Two peaks were separately collected at the *tR* = 4.568 min (9-*R*) and *tR* = 5.981 min (9-*S*) and the enantiomeric excess (e.e.) value of each product was above 99% (Figure 5). Like compound **7a**, the conformer 9-(*S*)-**14b** presented a superior RXFP4 agonism over that of 9-*R* (Efficacy = 134.4±5.2% and 27.8±8.9% for 9-*S* and 9-*R*, respectively), accompanied by an improved RXFP4 selective ratio *vs*. RXFP3 (from 4.8 for 9-(*S*)-**7a** to 26.9 for 9-(*S*)-**14b**). Compound **14c** exhibited agonist effects on both RXFP4 and RXFP3, which may result from the cytotoxicity (Figure S2).

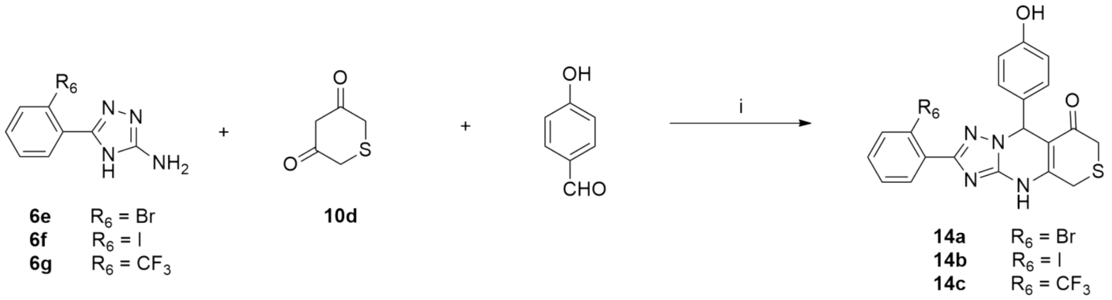

Scheme 3. Synthetic route for compounds **14a-c**. (i) HOAc in EtOH, reflux, yield: 41-51%.

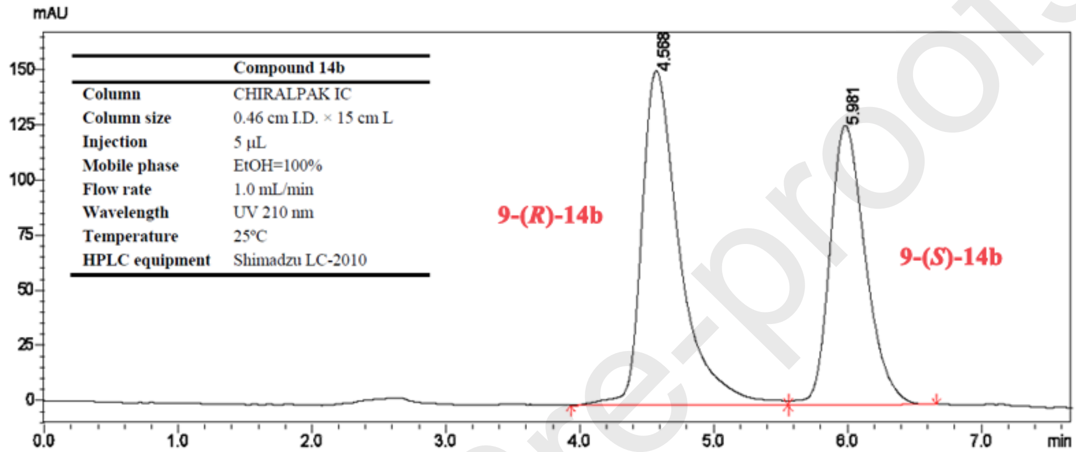

Figure 5. Chiral resolution of compound 14b. The condition of chiral resolution and its chromatography.

2.6. Receptor binding

Representative analogues 9-(*S*)-**7a**, **7e**, **7g**, **14a**, **14b** and 9-(*S*)-**14b** that exhibited better agonistic effects in cAMP accumulation assay were selected for the following competitive binding assay in CHO-K1 cells stably expressing human RXFP4 with europium-labeled Eu(A)-R3/I5 as control. The 9-(*R*) conformers of **7a** and **14b** were also tested in the binding assay as comparison. The results showed that 9-(*S*)-**7a** and 9-(*S*)-**14b** displayed superior binding affinity to their corresponding 9-(*R*)-conformers. However, their displacement curves were not paralleled with that of peptide R3/I5, indicating that only parts of the binding site for R3/I5 were competitively bound by the ligands. It was noted that 9-(*R*)-**7a** showed an increased binding effect which might be caused by the cell toxicity at high concentration (100 μM).

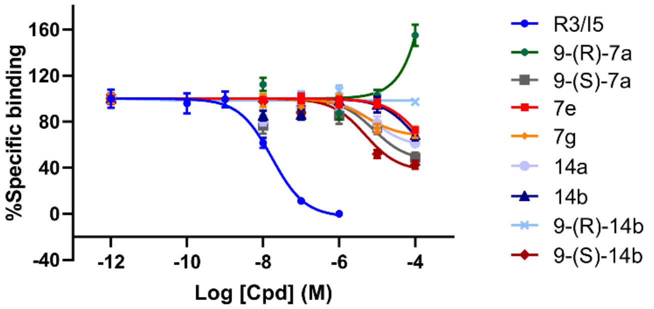

Compound	pKi
R3/I5	8.31 ± 0.10
9-(*S*)-7a	5.64 ± 0.28
7e	4.45 ± 0.90
7g	5.82 ± 0.28
14a	5.62 ± 0.27
14b	4.53 ± 0.99
9-(*S*)-14b	5.86 ± 0.15

Figure 6. Competitive binding assay of selected compounds with hRXFP4 performed in CHO-K1 cells stably expressing the receptor RXFP4. Europium-labeled Eu(A)-R3/I5 was used in the presence of increasing amounts of compounds. Each compound was measured in triplicate, and each experiment was repeated independently for three times. Data were analyzed using GraphPad PRISM 8 (GraphPad Inc., San Diego, CA) and expressed as means ± SEM.

2.7. Docking studies

Molecular docking was conducted using the Dock Ligands module of LibDock genetic algorithm program in BIOVIA Discovery Studio 2016 (Accelrys Software, San Diego, USA). Homology models of hRXFP4 and hRXFP3 (SWISS-MODEL: Q8TDU9 and Q9NSD7, respectively), modeled on the template of agonist-bound apelin receptor (PDB code: 5VBL), were used because the apelin receptor is also determined with agonist. The sequence identity between RXFP3/RXFP4 and apelin receptor is 32.1% and 28.2%, respectively. The proteins were prepared before docking and then cavity searching was performed to find the orthosteric binding site, which showed the best pocket score. Next, ligands were prepared using energy minimization by CHARMm forcefield until RMS gradient of 0.01 was reached. Compounds **7a** and **14b** were docked into the hRXFP4 orthosteric binding site constructed by residues L118$^{3.29}$, T176$^{4.60}$, R208$^{5.42}$, F291$^{7.35}$, Q205$^{5.39}$, T266$^{6.55}$, G269$^{6.58}$, V265$^{6.54}$, Q287$^{7.31}$, K273$^{6.62}$, Y284$^{7.28}$, T288$^{7.32}$, L201$^{5.35}$, P196$^{5.30}$, L193^{ECL2}, L192^{ECL2}, L190^{ECL2} and Y204$^{5.38}$, as well as the hRXFP3 orthosteric binding site constructed by residues T346$^{6.55}$, Y369$^{7.33}$, L345$^{6.54}$, L365$^{7.29}$, C366$^{7.30}$, S349$^{6.58}$, Y267$^{5.38}$, L264$^{5.35}$, I350$^{6.59}$, K353$^{6.62}$, F262^{ECL2}, W263$^{5.34}$, R250^{ECL2} and F251^{ECL2} (superscripts indicate Ballesteros-Weinstein numbering for GPCRs, [Ballesteros and Weinstein, 1995]) with the top 10 poses presented and scored while keeping other options in their default values (Figures 7 and S4). LibDock fitness scores of 114.064 and 111.977 with peptide RXFP4, and 111.545 and 111.749 with peptide RXFP3 for **7a** and **14b** were then obtained respectively. After binding to RXFP4, the phenolic hydroxyl group and nitrogen atom on the 1,2,4-triazole interacted *via* hydrogen bonds with the carbonyl group of L193^{ECL2} and the terminal amide of Q205$^{5.39}$, separately. Two aromatic rings (2-Cl/I-Ph and 1,2,4-triazole) formed Pi-Pi stack with F291$^{7.35}$. The aromatic rings (2-Cl/I-Ph) also formed Pi-cation function with the terminal amino group of K273$^{6.62}$. In addition, the sulfur atom on the thiopyrano ring of compound **14b** interacted with the phenolic ring of Y204$^{5.38}$, which may explain the efficacy difference between **14b** and **7a**. As comparison, docking studies of **7a** and **14b** with RXFP3 indicated that no hydrogen bond was formed between the peptide and ligands except for Pi-Pi stack, Pi-cation and Pi-sulfur functions. This may be interpreted as the selectivity of ligands for RXFP4 *vs.* RXFP3.

A

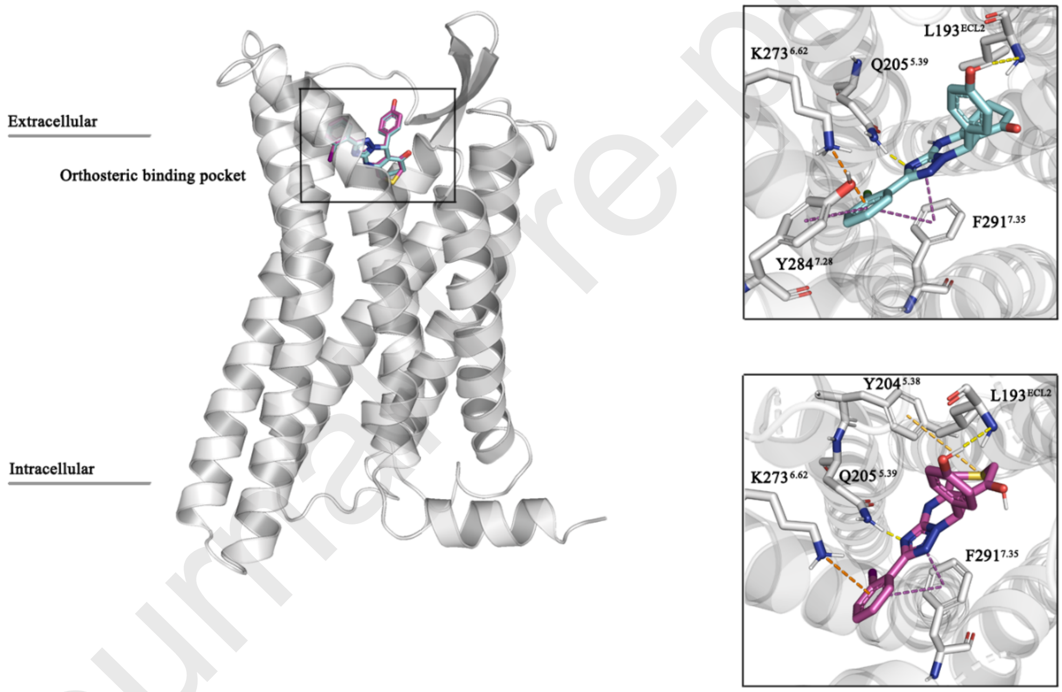

B

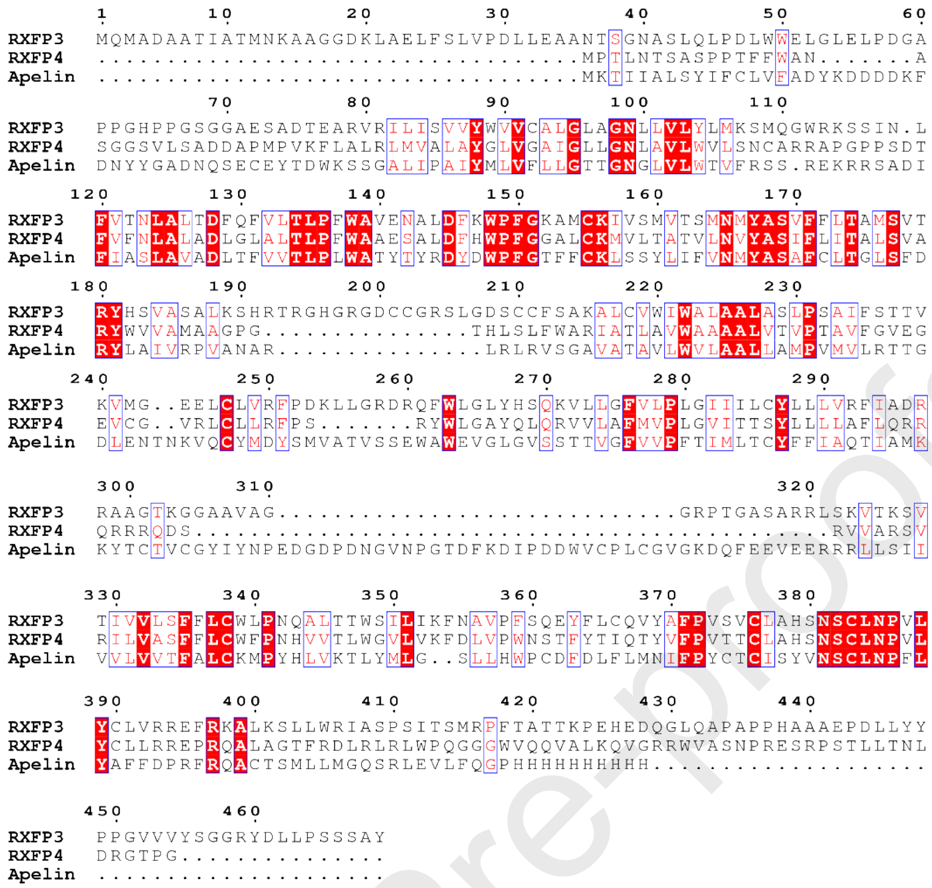

Figure 7. A, Molecular docking of compounds **7a** and **14b** with hRXFP4 (SWISS-MODEL: Q8TDU9) at the orthosteric binding site. Compounds **7a** and **14b** were displayed as cyan and pink sticks, respectively, while the amino acids of RXFP4 are shown as grey cartoon or sticks; **B**, Sequence alignment among RXFP3 (SWISS-MODEL: Q9NSD7), RXFP4 and apelin receptor (PDB code: 5VBL).

3. Conclusions

A new scaffold of tricyclic derivatives represented by **7a** as non-peptidic selective RXFP4 agonist was disclosed after HTS, capable of suppressing forskolin-stimulated cAMP production in hRXFP4-overexpressing CHO-K1 cells as opposed to hRXFP3 and hRXFP1. A pair of enantiomers (9-*R* and 9-*S*) was resolved and their structures were confirmed by X-ray crystallography. Medicinal chemistry efforts in modification of **7a** was then performed focusing on three parts: 2-chlorophenyl group, 4-hydroxyphenyl group and its skeleton including cyclohexane-1,3-dione and 1,2,4-triazole group. Initial optimization revealed that 2-bromophenyl, 2-iodophenyl and 2-trifluoromethylphenyl substitutes are superior to 2-chlorophenyl, 4-hydroxyphenyl is an essential group for receptor selectivity, the skeleton of 5,6,7,9-tetrahydro-[1,2,4]triazolo[5,1-b]quinazolin-8(4*H*)-one could be changed to 7,9-dihydro-4H-thiopyrano[3,4-d][1,2,4]triazolo[1,5-a]pyrimidin-8(5*H*)-one without loss of agonist activity on RXFP4 and 3-phenyl-1,2,4-triazole skeleton is a key functional group for RXFP4 binding. Based on this, our follow-up optimization resulted in 9-(*S*)-**14b** with 2.3-fold higher efficacy and better selectivity (selective ratio of RXFP4 *vs.* RXFP3 for 9-(*S*)-**14b** and **7a** were 26.9 and 13.9, respectively). Subsequent molecular docking was carried out to elucidate a possible reason of this selectivity for RXFP4 *vs*. RXFP3. Competitive binding assay of representative compounds were performed which further demonstrated 9-(*S*)-**14b** as the most potent RXFP4 agonist with a pKi value of 5.86 ± 0.15.

4. Experimental protocols

4.1. Chemistry

Reagents are of commercial grade and were used as received unless otherwise noted. The structures of all new compounds are consistent with their ^{1}H, ^{13}C NMR and mass spectra, and are judged to be ≥95% pure by HPLC. NMR spectra were recorded on Bruker AN-400, AVANCE III 500 and Varian Inova 600 spectrometers. Chemical shifts were reported in parts per million (ppm), with the solvent resonance as the internal standard (CD_3OD 3.31 ppm, $CDCl_3$ 7.26 ppm and DMSO-d_6 2.50 ppm for ^{1}H NMR; CD_3OD 49.15 ppm, $CDCl_3$ 77.23 ppm and DMSO-d_6 39.52 ppm for ^{13}C NMR). Low resolution mass spectral data (electrospray ionization) were acquired on a Finnigan LCQ-DECA mass spectrometer. High resolution mass spectral data were collected on Agilent G6520 Q-TOF mass spectrometer. Samples were analyzed for purity on a HP1100 series equipped with a Zorbax SB-C18 column (5 µm, 4.6 mm × 250 mm). Purities of final compounds were determined using a 5 µL injection with quantitation by AUC at 210 and 254 nm (Agilent diode array detector). X-ray diffraction was recorded on a Bruker D8 VENTURE single-crystal diffractometer. Specific optical rotation was determined on Autopol VI-Rudolph polarimeter. All the melting points of synthesized compounds were measured on WRS-1B digital melting point apparatus. The procedures for compounds **4-5** were included in Supplementary Information.

4.1.1. Synthesis of 3-Amine-5-(2-chlorophenyl)-4H-1,2,4-triazol (**6a**)

N-(2-Chlorobenzamido)-guanidine (**5a**, 997.7 mg, 4.71 mmol, 1 eq) and *p*-toluenesulfonic acid monohydrate (116.2 mg, 0.61 mmol, 0.13 eq) were dissolved in a mixture of water (28 mL) and dioxane (14 mL). The resulted solution was refluxed overnight. After cooling, it was filtered and the solution was evaporated *in vacuo* into a small amount, which was placed at room temperature (RT) for 1 h. The product was precipitated and then filtered as white powder (1.33 g, yield: 95.0 %). m.p. 222-223°C LR-ESI: 195.1 $[M+H]^+$. HR-ESI *m/z* calcd for $C_8H_8ClN_4$ $[M+H]^+$ 195.0437, found 195.0439. ^1H NMR (CD_3OD, 400 MHz) 7.37 (t, J = 7.6 Hz, 1H, phenyl C_4-H), 7.41 (dt, J = 1.6 Hz, J = 7.2 Hz, 1H, phenyl C_5-H), 7.50 (dd, J = 1.2 Hz, J = 7.6 Hz, 1H, phenyl C_3-H), 7.64 (dd, J = 2.0 Hz, J = 7.6 Hz, 1H, phenyl C_6-H). ^{13}C NMR (CD_3OD, 125 MHz) 128.1 (phenyl C_5), 131.4 (phenyl C_6), 131.7 (phenyl C_2), 132.6 (phenyl $C_{3,4}$), 134.2 (phenyl C_1), 155.9 (CNH_2), 157.2 (CN_1N_3).

The procedures for compounds **6b-m** are the same as **6a**.

4.1.2. 5-(3-Chlorophenyl)-4H-1,2,4-triazol-3-amine (**6b**)

Yield: 76.2 %, white powder, m.p. 200-202°C. LR-ESI: 195.1 $[M+H]^+$. HR-ESI *m/z* calcd for $C_8H_8ClN_4$ $[M+H]^+$ 195.0437, found 195.0436. ^1H NMR (CD_3OD, 400 MHz) 7.40 (m, 2H, phenyl $C_{4,5}$-H), 7.82 (d, J = 6.0 Hz, 1H, phenyl C_6-H), 7.91 (s, 1H, phenyl C_2-H). ^{13}C NMR (CD_3OD, 100 MHz) 125.5 (phenyl C_6), 127.1 (phenyl C_2), 130.2 (phenyl C_4), 131.3 (phenyl C_5), 134.2 (phenyl C_1), 135.7 (phenyl C_3), 159.1 (CNH_2), 159.7 (CN_1N_3).

4.1.3. 5-(4-Chlorophenyl)-4H-1,2,4-triazol-3-amine (**6c**)

Yield: 74.5 %, white powder, m.p. 227-229°C. LR-ESI: 195.1 $[M+H]^+$. HR-ESI *m/z* calcd for $C_8H_8ClN_4$ $[M+H]^+$ 195.0437, found 195.0436. ^1H NMR (CD_3OD, 400 MHz) 7.42 (d, J = 8.4 Hz, 2H, phenyl $C_{3,5}$-H), 7.88 (d, J = 8.4 Hz, 2H, phenyl $C_{2,6}$-H). ^{13}C NMR (CD_3OD, 100 MHz) 128.7 (phenyl $C_{2,6}$), 129.9 (phenyl $C_{3,5}$), 132.1 (phenyl C_1), 136.2 (phenyl C_4), 158.8 (CNH_2), 159.3 (CN_1N_3).

4.1.4. 5-(2-Fluorophenyl)-4H-1, 2, 4-triazol-3-amine (**6d**)

Yield: 90.0 %, white powder, m.p. 188-189°C. LR-ESI: 179.0 $[M+H]^+$. HR-ESI *m/z* calcd for $C_8H_8FN_4$ $[M+H]^+$ 179.0733, found 179.0732. ^1H NMR (CD_3OD, 400 MHz) 7.23 (m, 2H, phenyl $C_{4,5}$-H), 7.44 (m, 1H, phenyl C_6-H), 7.87 (t, J = 7.6 Hz, 1H, phenyl C_3-H). ^{13}C NMR (CD_3OD, 125 MHz) 117.3 (phenyl C_3), 119.6 (phenyl C_1), 125.5 (phenyl C_5), 131.0 (phenyl C_4), 132.3 (phenyl C_6), 160.6 (CNH_2), 162.6 (phenyl C_2, CN_1N_3).

4.1.5. 5-(2-Bromophenyl)-4H-1, 2, 4-triazol-3-amine (**6e**)

Yield: 87.5 %, m.p. 227-228°C. LR-ESI: 238.8 $[M+H]^+$. HR-ESI *m/z* calcd for $C_8H_8BrN_4$ $[M+H]^+$ 238.9932, found 238.9932. ^1H NMR (CD_3OD, 400 MHz) 7.33 (t, J = 7.6 Hz, 1H, phenyl C_5-H), 7.42 (t, J = 7.6 Hz, 1H, phenyl C_4-H), 7.57 (d, J = 7.6 Hz, 1H, phenyl C_3-H), 7.69 (d, J = 8.0 Hz, 1-H, phenyl C_3-H). ^{13}C NMR (CD_3OD, 125 MHz) 123.5 (phenyl C_2), 128.6 (phenyl C_5), 132.8 (phenyl $C_{4,6}$), 134.6 (phenyl C_3), 137.8

(phenyl C_1), 157.2 (CNH_2), 158.5 (CN_1N_3).

4.1.6. 5-(2-Iodophenyl)-4H-1, 2, 4-triazol-3-amine (**6f**)

Yield: 97.0 %, m.p. 240-242°C. LR-ESI: 287.0 $[M+H]^+$. HR-ESI *m/z* calcd for $C_8H_8IN_4$ $[M+H]^+$ 286.9794, found 286.9795. ^1H NMR (CD_3OD, 400 MHz) 7.10 (t, J = 7.2 Hz, 1H, phenyl C_5-H), 7.28 (d, J = 8.4 Hz, 1H, phenyl C_6-H), 7.47 (d, J = 7.6 Hz, 1H, phenyl C_4-H), 7.74 (d, J = 8.0 Hz, 1H, phenyl C_3-H).

4.1.7. 5-(2-Trifluoromethylphenyl)-4H-1, 2, 4-triazol-3-amine (**6g**)

Yield: 81.6 %, m.p. 165-167°C. LR-ESI: 228.9 $[M+H]^+$. HR-ESI *m/z* calcd for $C_9H_8F_3N_4$ $[M+H]^+$ 229.0701, found 229.0702. ^1H NMR (CD_3OD, 400 MHz) 7.63 (m, 2H, phenyl $C_{4,5}$-H), 7.68 (d, J = 6.8 Hz, 1H, phenyl C_3-H), 7.80 (d, J = 7.6 Hz, 1H, phenyl C_6-H). ^{13}C NMR (CD_3OD, 125 MHz) 127.5 (CF_3), 130.3 (phenyl C_2), 130.5 (phenyl C_1), 133.0 (phenyl $C_{3,4}$), 133.1 (phenyl $C_{5,6}$), 157.8 (CNH_2), 158.8 (CN_1N_3).

4.1.8. 5-(3-Methoxyphenyl)-4H-1,2,4-triazol-3-amine (**6h**)

Yield: 79.1 %, white powder, m.p. 223-225°C. LR-ESI: 191.1 $[M+H]^+$. HR-ESI *m/z* calcd for $C_9H_{11}N_4O$ $[M+H]^+$ 191.0933, found 191.0930. ^1H NMR (CD_3OD, 400 MHz) 3.84 (s, 3H, OCH_3), 6.96 (d, J = 8.4 Hz, 1H, phenyl C_4-H), 7.32 (t, J = 8.4 Hz, 1H, phenyl C_5-H), 7.48 (m, 2H, phenyl $C_{2,6}$-H). ^{13}C NMR (CD_3OD, 125 MHz) 55.9 (OCH_3), 112.4 (phenyl C_2), 116.5 (phenyl C_4), 119.6 (phenyl C_6), 130.8 (phenyl C_5), 133.1 (phenyl C_1), 159.9 (CNH_2), 161.5 (2C, OCH_3, CN_1N_3).

4.1.9. 5-(4-Methoxyphenyl)-4H-1,2,4-triazol-3-amine (**6i**)

Yield: 87.4 %, white powder, m.p. 224-226°C. LR-ESI: 191.2 $[M+H]^+$. HR-ESI *m/z* calcd for $C_9H_{11}N_4O$ $[M+H]^+$ 191.0933, found 191.0930. ^1H NMR (CD_3OD, 500 MHz) 3.83 (s, 3H, OCH_3), 6.97 (d, J = 8.0 Hz, 2H, phenyl $C_{3,5}$-H), 7.82 (d, J = 8.5 Hz, 2H, phenyl $C_{2,6}$-H). ^{13}C NMR (CD_3OD, 125 MHz) 56.0 (OCH_3), 115.2 (2C, phenyl $C_{3,5}$), 124.6 (phenyl C_1), 128.8 (2C, phenyl $C_{2,6}$), 149.1 (CNH_2), 152.3 (CN_1N_3), 159.4 (phenyl C_4).

4.1.10. 5-(2, 3-Dichlorophenyl)-4H-1, 2, 4-triazol-3-amine (**6j**)

Yield: 82.1%, white powder, m.p. 243-245°C. LR-ESI: 229.0 $[M+H]^+$. HR-ESI *m/z* calcd for $C_8H_7C_{l2}N_4$ $[M+H]^+$ 229.0048, found 229.0046. ^1H NMR (CD_3OD, 400 MHz) 7.36 (t, J = 7.6 Hz, 1H, phenyl C_5-H), 7.57 (d, J = 7.6 Hz, 1H, phenyl C_6-H), 7.61 (d, J = 8.0 Hz, 1H, phenyl C_4-H). ^{13}C NMR (CD_3OD, 125 MHz) 128.8 (phenyl C_6), 131.1 (2C, phenyl $C_{4,5}$), 132.4 (phenyl C_2), 132.7 (phenyl C_3), 135.0 (phenyl C_1), 158.6 (CNH_2), 158.9 (CN_1N_3).

4.1.11. 5-(2, 4-Dichlorophenyl)-4H-1, 2, 4-triazol-3-amine (**6k**)

Yield: 89.8 %, white powder, m.p. 242-243°C. LR-ESI: 229.0 $[M+H]^+$. HR-ESI *m/z* calcd for $C_8H_7C_{l2}N_4$ $[M+H]^+$ 229.0048, found 229.0046. ^1H NMR (CD_3OD, 400MHz) 7.41 (dd, J = 1.6 Hz, J = 8.4 Hz, 1H, phenyl C_5-H), 7.58 (s, 1H, phenyl C_3-H), 7.66 (d, J = 8.4 Hz, 1H, phenyl C_6-H). ^{13}C NMR (CD_3OD, 125 MHz) 128.4 (phenyl C_5), 131.2 (phenyl C_6), 133.6 (phenyl C_3), 135.1(2C, phenyl $C_{2,4}$), 136.7 (phenyl C_1), 158.4 (CNH_2), 159.3 (CN_1N_3).

4.1.12. 5-(2, 5-Dichlorophenyl)-4H-1, 2, 4-triazol-3-amine (**6l**)

Yield: 87.0 %, white powder, m.p. 268-269°C. LR-ESI: 229.1 $[M+H]^+$. HR-ESI *m/z* calcd for $C_8H_7C_{l2}N_4$ $[M+H]^+$ 229.0048, found 229.0047. ^1H NMR (CD_3OD, 400 MHz) 7.42 (d, J = 8.8 Hz, 1H, phenyl C_3-H), 7.49 (d, J = 8.8 Hz, 1H, phenyl C_4-H), 7.70 (s, 1H, phenyl C_6-H). ^{13}C NMR (CD_3OD, 125 MHz) 130.3 (phenyl C_2), 131.4 (phenyl C_6), 132.1 (phenyl C_4), 132.6 (phenyl C_5), 133.0 (phenyl C_3), 133.8 (phenyl C_1), 157.1 (CNH_2), 158.3 (CN_1N_3).

4.1.13. 5-Phenyl-4H-1,2,4-triazol-3-amine (**6m**)

Yield: 90.0 %, white powder, m.p. 187-188°C. LR-ESI: 161.1 $[M+H]^+$. HR-ESI *m/z* calcd for $C_8H_9N_4$ $[M+H]^+$ 161.0827, found 161.0827. ^1H NMR (CD_3OD, 400 MHz) 7.40 (m, 3H, phenyl $C_{3,4,5}$-H), 7.89 (d, J = 6.8 Hz, 2H, phenyl $C_{2,6}$-H). ^{13}C NMR (CD_3OD, 125 MHz) 127.3 (2C, phenyl $C_{2,6}$), 129.8 (2C, phenyl $C_{3,5}$), 130.5 (phenyl C_4), 131.9 (phenyl C_1), 159.9 (CNH_2), 160.2 (CN_1N_3).

4.1.14. Synthesis of 2-(2-Chlorophenyl)-9-(4-hydroxyphenyl)-5,6,7,9-tetrahydro-[1,2,4]triazolo[5,1-b] quinazolin-8(4H)-one (**7a**)

Acetic acid (600 μL) was added to the solution of 5-(2-chloro)phenyl-4*H*-1,2,4-triazol-3-amine (**6a**, 4 g, 20.6 mmol, 1 eq), cyclohexane-1,3-dione (2.3 g, 20.6 mmol, 1 eq) and 4-hydroxybenzaldehyde (2.5 g, 20.6 mmol, 1 eq) in EtOH (130 mL). The reaction was refluxed overnight. After cooling, the solvent was removed *in vacuo* and the residue was separated on the Biotage® SNAP Cartridge Sil-100g column eluting with 0-10% methanol/dichloromethane to obtain the product as yellowish powder (1.8 g, yield: 32.3 %). m.p. 297-298°C. LR-ESI: 391.2 $[M-H]^-$. HR-ESI *m/z* calcd for $C_{21}H_{16}ClN_4O_2$ $[M-H]^-$ 391.0962, found 391.0968. ^1H NMR (CD_3OD, 500 MHz) 2.05 (m, 1H, C_6-H), 2.10 (m, 1H, C_6-H), 2.40 (m, 2H, C_5-H), 2.75 (m, 2H, C_7-H), 6.34 (s, 1H, C_9-H), 6.70 (d, J = 8.5 Hz, 2H, 4-OH phenyl $C_{3,5}$-H), 7.14 (d, J = 9.0 Hz, 2H, 4-OH phenyl $C_{2,6}$-H), 7.33 (dt, J = 1.0 Hz, J = 7.5 Hz, 1H, 2-Cl phenyl C_5-H), 7.38 (dt, J = 1.0 Hz, J = 7.5 Hz, 1H, 2-Cl phenyl C_4-H), 7.47 (dd, J = 1.0 Hz, J = 7.5 Hz, 1H, 2-Cl phenyl C_3-H), 7.63 (dd, J = 2.0 Hz, J = 8.0 Hz, 1H, 2-Cl phenyl C_6-H). ^{13}C NMR

(CD_3OD, 125 MHz) 22.3 (C_6), 28.0 (C_7), 37.7 (C_5), 59.4 (C_9), 109.8 (C_{8a}), 116.3 (2C, 4-OH phenyl $C_{3,5}$), 128.0 (2-Cl phenyl C_5), 129.6 (2C, 4-OH phenyl $C_{2,6}$), 131.5 (2C, 2-Cl phenyl $C_{1,3}$), 131.8 (2-Cl phenyl C_4), 132.7 (2-Cl phenyl C_6), 133.6 (4-OH phenyl C_1), 134.3 (2-Cl phenyl C_2), 148.8 (C_{5a}), 154.5 (CN_2N_4), 158.6 (4-OH phenyl C_4), 160.2 (CN_1N_3), 197.2 (CO).

Compounds **7b-m**, **9a-i**, **11a-d**, **13a-c** and **14a-c** were prepared using similar procedures as compound **7a**.

4.1.15. 2-(3-Chlorophenyl)-9-(4-hydroxyphenyl)-5,6,7,9-tetrahydro-[1,2,4]triazolo[5,1-b]quinazolin- 8(4H)-one (**7b**)

Yield: 43.3%, yellowish powder. m.p. 297-299°C. LR-ESI: 391.1 $[M-H]^-$. HR-ESI *m/z* calcd for $C_{21}H_{16}ClN_4O_2$ $[M-H]^-$ 391.0962, found 391.0962. ^1H NMR (CD_3OD, 500 MHz) 2.03 (m, 1H, C_6-H), 2.11 (m, 1H, C_6-H), 2.40 (m, 2H, C_5-H), 2.78 (m, 2H, C_7-H), 6.30 (s, 1H, C_9-H), 6.71 (d, J = 8.5 Hz, 2H, 4-OH phenyl $C_{3,5}$-H), 7.14 (d, J = 8.5 Hz, 2H, 4-OH phenyl $C_{2,6}$-H), 7.37 (m, 2H, 3-Cl phenyl $C_{4,5}$-H), 7.86 (m, 1H, 3-Cl phenyl C_6-H), 7.93 (s, 1H, 3-Cl phenyl C_2-H). ^{13}C NMR (CD_3OD, 125 MHz) 22.3 (C_6), 28.0 (C_5), 37.7 (C_7), 56.0 (C_9), 109.8 (C_{8a}), 116.3 (2C, 4-OH phenyl $C_{3,5}$), 125.6 (3-Cl phenyl C_6), 127.2 (3-Cl phenyl C_2), 129.6 (2C, 4-OH phenyl $C_{2,6}$), 130.4 (3-Cl phenyl C_4), 131.3 (3-Cl phenyl C_5), 133.7 (4-OH phenyl C_1), 134.1 (3-Cl phenyl C_1), 135.7 (3-Cl phenyl C_3), 151.4 (C_{5a}), 154.5 (CN_2N_4), 159.2 (4-OH phenyl C_4), 160.4 (CN_1N_3), 197.3 (CO).

4.1.16. 2-(4-Chlorophenyl)-9-(4-hydroxyphenyl)-5,6,7,9-tetrahydro-[1,2,4]triazolo[5,1-b]quinazolin- 8(4H)-one (**7c**)

Yield: 33.4%, yellowish powder. m.p. 297-298°C. LR-ESI: 391.2 $[M-H]^-$. HR-ESI *m/z* calcd for $C_{21}H_{16}ClN_4O_2$ $[M-H]^-$ 391.0962, found 391.0954. ^1H NMR (CD_3OD, 400 MHz) 2.03 (m, 1H, C_6-H), 2.10 (m, 1H, C_6-H), 2.40 (m, 2H, C_5-H), 2.76 (m, 2H, C_7-H), 6.29 (s, 1H, C_9-H), 6.70 (d, J = 8.4 Hz, 2H, 4-OH phenyl $C_{3,5}$-H), 7.12 (d, J = 8.4 Hz, 2H, 4-OH phenyl $C_{2,6}$-H), 7.39 (d, J = 8.4 Hz, 2H, 4-Cl phenyl $C_{3,5}$-H), 7.91 (d, J = 8.8 Hz, 2H, 4-Cl phenyl $C_{2,6}$-H). ^{13}C NMR (CD_3OD, 125 MHz) 22.2 (C_6), 28.0 (C_5), 37.7 (C_7), 59.5 (C_9), 109.8 (C_{8a}), 116.3 (2C, 4-OH phenyl $C_{3,5}$), 128.9 (2C, 4-Cl phenyl $C_{2,6}$), 129.6 (2C, 4-Cl phenyl $C_{3,5}$), 129.9 (2C, 4-OH phenyl $C_{2,6}$), 130.9 (4-OH phenyl C_1), 133.8 (4-Cl phenyl C_1), 136.4 (4-Cl phenyl C_4), 149.3 (C_{5a}), 154.5 (CN_2N_4), 158.6 (4-OH phenyl C_4), 160.8 (CN_1N_3), 197.3 (CO).

4.1.17. 2-(2-Fluorophenyl)-9-(4-hydroxyphenyl)-5,6,7,9-tetrahydro-[1,2,4]triazolo[5,1-b]quinazolin- 8(4H)-one (**7d**)

Yield: 52.8 %, yellowish powder, m.p. 263-264°C. LR-ESI: 375.2 $[M-H]^-$. HR-ESI *m/z* calcd for $C_{21}H_{16}FN_4O_2$ $[M-H]^-$ 375.1257, found 375.1256. ^1H NMR (CD_3OD, 400 MHz) 2.09 (m, 2H, C_6-H), 2.40 (m, 2H, C_5-H), 2.77 (m, 2H, C_7-H), 6.34 (s, 1H, C_9-H), 6.70 (d, J = 8.0 Hz, 2H, 4-OH phenyl $C_{3,5}$-H), 7.14 (d, J = 8.4 Hz, 2H, 4-OH phenyl $C_{2,6}$-H), 7.20 (m, 2H, 2-F phenyl $C_{5,6}$-H), 7.41 (m, 1H, 2-F phenyl C_4-H), 7.88 (t, J = 7.6 Hz, 1H, 2-F phenyl C_3-H). ^{13}C NMR (CD_3OD, 125 MHz) 22.3 (C_6), 28.0 (C_5), 37.7 (C_7), 59.4 (C_9), 110.0 (C_{8a}), 116.3 (2C, 4-OH phenyl $C_{3,5}$), 117.4 (2-F phenyl C_3), 120.1 (2-F phenyl C_1), 125.4 (2-F phenyl C_5), 129.6 (2C, 4-OH phenyl $C_{2,6}$), 131.4 (2-F phenyl C_6), 132.3 (2-F phenyl C_4), 133.7 (4-OH phenyl C_1), 149.0 (C_{5a}), 154.4 (CN_2N_4), 158.6 (4-OH phenyl C_4), 160.7 (2-F phenyl C_2), 162.7 (CN_1N_3), 197.2 (CO).

4.1.18. 2-(2-Bromophenyl)-9-(4-hydroxyphenyl)-5,6,7,9-tetrahydro-[1,2,4]triazolo[5,1-b]quinazolin- 8(4H)-one (**7e**)

Yield: 55.3 %, yellowish powder, m.p. >300°C. LR-ESI: 435.1 $[M-H]^-$, 437.1. HR-ESI *m/z* calcd for $C_{21}H_{16}BrN_4O_2$ $[M-H]^-$ 435.0457, found 435.0463. ^1H NMR (CD_3OD, 400 MHz) 2.03 (m, 2H, C_6-H), 2.37 (m, 2H, C_5-H), 2.69 (m, 2H, C_7-H), 6.33 (s, 1H, C_9-H), 6.71 (d, J = 8.0 Hz, 2H, 4-OH phenyl $C_{3,5}$-H), 7.14 (d, J = 8.0 Hz, 2H, 4-OH phenyl $C_{2,6}$-H), 7.28 (t, J = 7.6 Hz, 1H, 2-Br phenyl C_4-H), 7.36 (t, J = 7.2 Hz, 1H, 2-Br phenyl C_5-H), 7.55 (d, J = 7.6 Hz, 1H, 2-Br phenyl C_3-H), 7.64 (d, J = 7.6 Hz, 1H, 2-Br phenyl C_6-H). ^{13}C NMR (CD_3OD, 125 MHz) 22.2 (C_6), 28.0 (C_5), 37.7 (C_7), 59.3 (C_9), 109.7 (C_{8a}), 116.3 (2C, 4-OH phenyl $C_{3,5}$), 123.4 (2-Br phenyl C_2), 128.5 (2-Br phenyl C_5), 129.6 (2C, 4-OH phenyl $C_{2,6}$), 132.0 (2-Br phenyl C_6), 132.8 (2-Br phenyl C_3), 133.5 (4-OH phenyl C_1), 133.7 (2-Br phenyl C_1), 134.7 (2-Br phenyl C_3), 148.8 (C_{5a}), 154.7 (CN_2N_4), 158.6 (4-OH phenyl C_4), 161.2 (CN_1N_3), 197.2 (CO).

4.1.19. 2-(2-Iodophenyl)-9-(4-hydroxyphenyl)-5,6,7,9-tetrahydro-[1,2,4]triazolo[5,1-b]quinazolin- 8(4H)-one (**7f**)

Yield: 50.0 %, yellowish powder, m.p. >300°C. LR-ESI: 483.0 $[M-H]^-$. HR-ESI *m/z* calcd for $C_{21}H_{16}IN_4O_2$ $[M-H]^-$ 483.0318, found 483.0321. ^1H NMR (CD_3OD, 400 MHz) 2.05 (m, 2H, C_6-H), 2.38 (m, 2H, C_5-H), 2.69 (m, 2H, C_7-H), 6.32 (s, 1H, C_9-H), 6.70 (d, J = 8.0 Hz, 2H, 4-OH phenyl $C_{3,5}$-H), 7.14 (d, J = 7.6 Hz, 2H, 4-OH phenyl $C_{2,6}$-H), 7.39 (m, 2H, 2-I phenyl $C_{5,6}$-H), 7.47 (d, J = 7.6 Hz, 1H, 2-I phenyl C_4-H), 7.93 (d, J = 8.0 Hz, 1H, 2-I phenyl C_3-H). ^{13}C NMR (CD_3OD, 125 MHz) 22.2 (C_6), 28.0 (C_5), 37.7 (C_7), 59.4 (C_9), 109.9 (C_{8a}), 116.9 (2C, 4-OH phenyl $C_{3,5}$), 128.2 (2-I phenyl C_5), 129.2 (2-I phenyl C_6), 130.6 (2C, 4-OH phenyl $C_{2,6}$), 130.9 (2-I phenyl C_4), 132.0 (4-OH phenyl C_1), 132.3 (2-I phenyl C_3), 133.6 (2-I phenyl C_1), 133.8 (2-I phenyl C_2), 149.2 (C_{5a}), 154.5 (CN_2N_4), 158.5 (4-OH phenyl C_4), 161.8 (CN_1N_3), 197.3 (CO).

4.1.20. 2-(2-Trifluoromethylphenyl)-9-(4-hydroxyphenyl)-5,6,7,9-tetrahydro-[1,2,4]triazolo[5,1-b] quinazolin-8(4H)-one (**7g**)

Yield: 57.1 %, yellowish powder, m.p. >300°C. LR-ESI: 425.2 $[M-H]^-$. HR-ESI *m/z* calcd for $C_{22}H_{16}F_3N_4O_2$ $[M-H]^-$ 425.1225, found 425.1221. ^1H NMR (CD_3OD, 400 MHz) 2.10 (m, 2H, C_6-H), 2.41 (m, 2H, C_5-H), 2.77 (m, 2H, C_7-H), 6.33 (s, 1H, C_9-H), 6.71 (d, J = 8.0 Hz, 2H, 4-OH phenyl $C_{3,5}$-H), 7.12 (d, J = 7.6 Hz, 2H, 4-OH phenyl $C_{2,6}$-H), 7.63 (m, 3H, 2-CF_3 phenyl $C_{3,4,5}$-H), 7.77 (d, J = 7.2 Hz, 1H, 2-CF_3 phenyl C_6-H). ^{13}C NMR (CD_3OD, 125 MHz) 22.2 (C_6), 28.0 (C_5), 37.7 (C_7), 59.3 (C_9), 109.8 (C_{8a}), 116.2 (2C, 4-OH phenyl $C_{3,5}$), 124.4 (CF_3), 127.6 (2-CF_3 phenyl C_3), 129.5 (2C, 4-OH phenyl $C_{2,6}$), 130.3 (2-CF_3 phenyl C_2), 130.5 (4-OH phenyl C_1), 130.9 (2-CF_3 phenyl C_4), 133.0 (2-CF_3 phenyl C_6), 133.1 (2-CF_3 phenyl C_5), 133.5 (2-CF_3 phenyl C_1), 148.9 (C_{5a}), 154.6 (CN_2N_4), 158.5 (4-OH phenyl C_4), 160.4 (CN_1N_3), 197.3 (CO).

4.1.21. 2-(3-Methoxyphenyl)-9-(4-hydroxyphenyl)-5,6,7,9-tetrahydro-[1,2,4]triazolo[5,1-b] quinazolin-8(4H)-one (**7h**)

Yield: 52.8 %, white powder, m.p. 291-292°C. LR-ESI: 387.3 $[M-H]^-$. HR-ESI *m/z* calcd for $C_{22}H_{19}N_4O_3$ $[M-H]^-$ 387.1457, found 387.1455. ^1H NMR (CD_3OD, 400 MHz) 2.09 (m, 2H, C_6-H), 2.40 (m, 2H, C_5-H), 2.75 (m, 2H, C_7-H), 3.82 (s, 3H, OCH_3), 6.30 (s, 1H, C_9-H), 6.70 (d, J = 8.4 Hz, 2H, 4-OH phenyl $C_{3,5}$-H), 6.94 (dd, J = 2.0 Hz, J = 8.8 Hz, 1H, 3-OCH_3 phenyl C_4-H), 7.13 (d, J = 8.4 Hz, 2H, 4-OH phenyl $C_{2,6}$-H), 7.29 (t, J = 8.0 Hz, 1H, 3-OCH_3 phenyl C_5-H), 7.50 (d, J = 2.8 Hz, 1H, 3-OCH_3 phenyl C_2-H), 7.52 (d, J = 8.8 Hz, 1H, 3-OCH_3 phenyl C_6-H). ^{13}C NMR (CD_3OD, 125 MHz) 22.3 (C_6), 28.0 (C_5), 37.7 (C_7), 55.9 (OCH_3), 59.4 (C_9), 110.0 (C_{8a}), 112.4 (3-OCH_3 phenyl C_2), 116.3 (2C, 4-OH phenyl $C_{3,5}$), 116.7 (3-OCH_3 phenyl C_4), 119.8 (3-OCH_3 phenyl C_6), 129.6 (2C, 4-OH phenyl $C_{2,6}$), 130.8 (3-OCH_3 phenyl C_5), 133.3 (4-OH phenyl C_1), 133.8 (3-OCH_3 phenyl C_1), 149.2 (C_{5a}), 154.4 (CN_2N_4), 158.6 (4-OH phenyl C_4), 161.5 (CN_1N_3), 161.7 (3-OCH_3 phenyl C_3), 197.2 (CO).

4.1.22. 9-(4-Hydroxyphenyl)-2-(4-methoxyphenyl)-5,6,7,9-tetrahydro-[1,2,4]triazolo[5,1-b] quinazolin-8(4H)-one (**7i**)

Yield: 30.1%, yellowish powder. LR-ESI: 387.2 $[M-H]^-$. HR-ESI *m/z* calcd for $C_{22}H_{19}N_4O_3$ $[M-H]^-$ 387.1457, found 387.1457. ^1H NMR (CD_3OD, 400 MHz) 2.09 (m, 2H, C_6-H), 2.39 (m, 2H, C_5-H), 2.77 (m, 2H, C_7-H), 3.81 (s, 3H, OCH_3), 6.28 (s, 1H, C_9-H), 6.70 (d, J = 8.4 Hz, 2H, 4-OH phenyl $C_{3,5}$-H), 6.94 (d, J = 8.8 Hz, 2H, 4-OCH_3

phenyl $C_{3,5}$-H), 7.12 (d, J = 8.4 Hz, 2H, 4-OH phenyl $C_{2,6}$-H), 7.85 (d, J = 9.2 Hz, 2H, 4-OCH_3 phenyl $C_{2,6}$-H).

4.1.23. 2-(2,3-Dichlorophenyl)-9-(4-hydroxyphenyl)-5,6,7,9-tetrahydro-[1,2,4]triazolo[5,1-b] quinazolin-8(4H)-one (**7j**)

Yield: 50.6 %, yellowish powder, m.p. 280-281°C. LR-ESI: 425.1 $[M-H]^-$. HR-ESI *m/z* calcd for $C_{21}H_{15}Cl_2N_4O_2$ $[M-H]^-$ 425.0572, found 425.0574. ^1H NMR (CD_3OD, 400 MHz) 2.06 (m, 1H, C_6-H), 2.12 (m, 1H, C_6-H), 2.41 (m, 2H, C_5-H), 2.77 (m, 2H, C_7-H), 6.34 (s, 1H, C_9-H), 6.71 (d, J = 8.8 Hz, 2H, 4-OH phenyl $C_{3,5}$-H), 7.14 (d, J = 8.8 Hz, 2H, 4-OH phenyl $C_{2,6}$-H), 7.33 (t, J = 8.0 Hz, 1H, 2,3-di Cl phenyl C_5-H), 7.57 (d, J = 8.0 Hz, 1H, 2,3-di Cl phenyl C_6-H), 7.59 (d, J = 8.0 Hz, 1H, 2,3-di Cl phenyl C_4-H). ^{13}C NMR (CD_3OD, 125 MHz) 22.3 (C_6), 28.0 (C_5), 37.7 (C_7), 59.4 (C_9), 109.8 (C_{8a}), 116.3 (2C, 4-OH phenyl $C_{3,5}$), 128.8 (2,3-di Cl phenyl C_6), 129.6 (2C, 4-OH phenyl $C_{2,6}$), 131.2 (2,3-di Cl phenyl C_5), 132.5 (2,3-di Cl phenyl C_4), 133.5 (2,3-di Cl phenyl C_2), 133.9 (4-OH phenyl C_4), 135.0 (2,3-di Cl phenyl C_3), 135.1 (2,3-di Cl phenyl C_1), 148.8 (C_{5a}), 154.6 (CN_2N_4), 158.6 (4-OH phenyl C_4), 159.7 (CN_1N_3), 197.3 (CO).

4.1.24. 2-(2,4-Dichlorophenyl)-9-(4-hydroxyphenyl)-5,6,7,9-tetrahydro-[1,2,4]triazolo[5,1-b] quinazolin-8(4H)-one (**7k**)

Yield: 55.9 %, yellowish powder, m.p. 281-283°C. LR-ESI: 425.2 $[M-H]^-$. HR-ESI *m/z* calcd for $C_{21}H_{15}Cl_2N_4O_2$ $[M-H]^-$ 425.0572, found 425.0580. ^1H NMR (CD_3OD, 500 MHz) 2.03 (m, 1H, C_6-H), 2.09 (m, 1H, C_6-H), 2.39 (m, 2H, C_5-H), 2.75 (m, 2H, C_7-H), 6.33 (s, 1H, C_9-H), 6.70 (d, J = 8.5 Hz, 2H, 4-OH phenyl $C_{3,5}$-H), 7.13 (d, J = 8.5 Hz, 2H, 4-OH phenyl $C_{2,6}$-H), 7.36 (dd, J = 2.5 Hz, J = 8.5 Hz, 1H, 2,4-di Cl phenyl C_5-H), 7.52 (d, J = 2.0 Hz, 1H, 2,4-di Cl phenyl C_3-H), 7.67 (d, J = 8.5 Hz, 1H, 2,4-di Cl phenyl C_6-H). ^{13}C NMR (CD_3OD, 125 MHz) 22.2 (C_6), 28.0 (C_5), 37.7 (C_7), 59.4 (C_9), 109.7 (C_{8a}), 116.2 (2C, 4-OH phenyl $C_{3,5}$), 128.3 (2,4-di Cl phenyl C_5), 129.6 (2C, 4-OH phenyl $C_{2,6}$), 130.2 (2,4-di Cl phenyl C_2), 131.3 (2,4-di Cl phenyl C_6), 133.6 (2,4-di Cl phenyl C_4), 135.0 (4-OH phenyl C_1), 136.8 (2,4-di Cl phenyl C_1), 148.8 (C_{5a}), 154.6 (CN_2N_4), 158.6 (4-OH phenyl C_4), 159.3 (CN_1N_3), 197.2 (CO).

4.1.25. 2-(2,5-Dichlorophenyl)-9-(4-hydroxyphenyl)-5,6,7,9-tetrahydro-[1,2,4]triazolo[5,1-b] quinazolin-8(4H)-one (**7l**)

Yield: 61.4 %, yellowish powder, 283-284°C. LR-ESI: 425.1 $[M-H]^-$. HR-ESI *m/z* calcd for $C_{21}H_{15}Cl_2N_4O_2$ $[M-H]^-$ 425.0572, found 425.0578. ^1H NMR (DMSO-d_6, 400 MHz) 1.96 (m, 2H, C_6-H), 2.28 (m, 2H, C_5-H), 2.68 (m, 2H, C_7-H), 6.21 (s, 1H, C_9-H), 6.66 (d, J = 7.6 Hz, 2H, 4-OH phenyl $C_{3,5}$-H), 7.07 (d, J = 8.0 Hz, 2H, 4-OH phenyl $C_{2,6}$-H), 7.49 (d, J = 8.8 Hz, 1H, 2,5-di Cl phenyl C_4-H), 7.57 (d, J = 8.8 Hz , 1H, 2,5-di Cl phenyl C_3-H), 7.76 (brs, 1H, 2,5-di Cl phenyl C_6-H), 9.40 (s, OH), 11.26 (brs, NH). ^{13}C NMR (DMSO-d_6, 125 MHz) 20.6 (C_6), 26.4 (C_5), 36.3 (C_7), 57.3 (C_9), 107.0 (C_{8a}), 115.0 (2C, 4-OH phenyl $C_{3,5}$), 128.2 (2C, 4-OH phenyl $C_{2,6}$), 129.9 (2,5-di Cl phenyl C_6), 130.0 (4-OH phenyl C_1), 130.1 (2,5-di Cl phenyl C_4), 131.2 (2,5-di Cl phenyl C_2), 131.6 (2,5-di Cl phenyl C_5), 131.7 (C_{5a}), 132.4 (2,5-di Cl phenyl C_3), 147.1 (2,5-di Cl phenyl C_1), 152.1 (CN_2N_4), 156.5 (4-OH phenyl C_1), 157.0 (CN_1N_3), 193.2 (CO).

4.1.26. 2-(Phenyl)-9-(4-hydroxyphenyl)-5,6,7,9-tetrahydro-[1,2,4]triazolo[5,1-b]quinazolin-8(4H)- one (**7m**)

Yield: 60.4 %, yellowish powder, m.p. 260-262°C. LR-ESI: 357.2 [M-H]$^-$. HR-ESI m/z calcd for $C_{21}H_{17}N_4O_2$ [M-H]$^-$ 357.1352, found 357.1354. ^1H NMR (CD_3OD, 400 MHz) 2.07 (m, 2H, C_6-H) , 2.39 (m, 2H, C_5-H), 2.77 (m, 2H, C_7-H), 6.29 (s, 1H, C_9-H), 6.71 (d, J = 8.4 Hz, 2H, 4-OH phenyl $C_{3,5}$-H), 7.14 (d, J = 8.4 Hz, 2H, 4-OH phenyl $C_{2,6}$-H), 7.38 (m, 3H, phenyl $C_{3,4,5}$-H), 7.92 (m, 2H, phenyl $C_{2,6}$-H). ^{13}C NMR (CD_3OD, 125 MHz) 22.2 (C_6), 30.8 (C_5), 37.7 (C_7), 55.8 (C_9), 109.8 (C_{8a}), 116.2 (2C, 4-OH phenyl $C_{3,5}$), 127.3 (2C, phenyl $C_{2,6}$), 129.5 (4-OH phenyl C_1), 129.6 (2C, phenyl $C_{3,5}$), 129.7 (2C, 4-OH phenyl $C_{2,6}$), 130.1 (phenyl C_4), 133.8 (C_{5a}), 134.4 (phenyl C_1), 153.2 (CN_2N_4), 154.6 (4-OH phenyl C_4), 158.5 (CN_1N_3), 197.3 (CO).

4.1.27. 2-(2-Chlorophenyl)-9-(3-hydroxyphenyl)-5,6,7,9-tetrahydro-[1,2,4]triazolo[5,1-b]quinazolin- 8(4H)-one (**9a**)

Yield: 43.6 %, yellowish powder, m.p. 280-282°C. LR-ESI: 391.3 [M-H]$^-$. HR-ESI m/z calcd for $C_{21}H_{16}ClN_4O_2$ [M-H]$^-$ 391.0962, found 391.0960. ^1H NMR (CD_3OD, 400 MHz) 2.11 (m, 1H, C_6-H), 2.20 (t, J = 7.2 Hz, 1H, C_6-H), 2.42 (m, 2H, C_5-H), 2.78 (m, 2H, C_7-H), 6.36 (s, 1H, C_9-H), 6.67 (d, J = 8.4 Hz, 1H, 3-OH phenyl C_4-H), 6.75 (s, 1H, 3-OH phenyl C_2-H), 6.78 (d, J = 7.6 Hz, 1H, 3-OH phenyl C_6-H), 7.11 (t, J = 8.0 Hz, 1H, 3-OH phenyl C_5-H), 7.34 (t, J = 7.6 Hz, 1H, 2-Cl phenyl C_4-H), 7.39 (t, J = 7.6 Hz, 1H, 2-Cl phenyl C_5-H), 7.47 (d, J = 7.6 Hz, 1H, 2-Cl phenyl C_3-H) , 7.65 (d, J = 6.8 Hz, 1H, 2-Cl phenyl C_6-H). ^{13}C NMR (CD_3OD, 125 MHz) 22.1 (C_6), 28.0 (C_5), 37.7 (C_7), 59.6 (C_9), 109.6 (C_{8a}), 115.2 (3-OH phenyl C_4), 116.2 (3-OH phenyl C_2), 119.5 (3-OH phenyl C_6), 128.0 (2-Cl phenyl C_5), 130.6 (2-Cl phenyl C_6), 131.5 (2-Cl phenyl C_3), 131.8 (3-OH phenyl C_5), 132.7 (2-Cl phenyl C_4), 134.3 (2-Cl phenyl C_2), 138.6 (2-Cl phenyl C_1), 139.0 (C_{5a}), 143.8 (3-OH phenyl C_1), 148.9 (CN_2N_4), 154.8 (3-OH phenyl C_3), 158.8 (CN_1N_3), 197.2 (CO).

4.1.28. 2-(2-Chlorophenyl)-9-cyclohexyl-5,6,7,9-tetrahydro-[1,2,4]triazolo[5,1-

b]quinazolin-8(4H)- one (**9b**)

Yield: 59.2%, white powder. LR-ESI: 381.2 [M-H]$^-$. HR-ESI *m/z* calcd for $C_{21}H_{22}ClN_4O$ [M-H]$^-$ 381.1482, found 381.1485. ^{1}H NMR (CD_3OD, 400 MHz) 1.02 (m, 1H, cyclohexyl C_1-H), 1.17 (m, 2H, cyclohexyl $C_{2,6}$-H), 1.66 (m, 8H, cyclohexyl), 2.07 (m, 2H, C_6-H), 2.45 (m, 2H, C_5-H), 2.66 (brs, 2H, C_7-H), 5.30 (s, 1H, C_9-H), 7.39 (m, 2H, 2-Cl phenyl $C_{4,5}$-H), 7.50 (d, J = 7.2 Hz, 1H, 2-Cl phenyl C_3-H), 7.72 (d, J = 6.8 Hz, 1H, 2-Cl phenyl C_6-H). ^{13}C NMR (CD_3OD, 125 MHz) 22.2 (C_6), 27.4 (cyclohexyl C_3), 27.5 (cyclohexyl C_5), 27.6 (cyclohexyl C_4), 27.8 (cyclohexyl C_2), 27.9 (cyclohexyl C_6), 32.4 (C_5), 37.8 (C_7), 46.7 (cyclohexyl C_1), 60.6 (C_9), 108.1 (C_{8a}), 128.0 (2-Cl phenyl C_5), 131.5 (2-Cl phenyl C_6), 131.6 (2-Cl phenyl C_2), 131.7 (2-Cl phenyl C_3), 132.6 (2-Cl phenyl C_4), 134.3 (2-Cl phenyl C_1), 149.9 (C_{5a}), 156.4 (CN_2N_4), 159.3 (CN_1N_3), 197.6 (CO).

4.1.29. 2-(2-Chlorophenyl)-9-(3,4-dihydroxyphenyl)-5,6,7,9-tetrahydro-[1,2,4]triazolo[5,1-b] quinazolin-8(4H)-one (**9c**)

Yield: 61.3 %, yellowish powder, m.p. 298-300°C. LR-ESI: 407.1 [M-H]$^-$. HR-ESI *m/z* calcd for $C_{21}H_{16}ClN_4O_3$ [M-H]$^-$ 407.0911, found 407.0916. ^{1}H NMR (CD_3OD, 400 MHz) 2.04 (m, 2H, C_6-H), 2.40 (brs, 2H, C_5-H), 2.74 (brs, 2H, C_7-H), 6.28 (s, 1H, C_9-H), 6.66 (d, J = 8.4 Hz, 1H, 3,4-di OH phenyl C_6-H), 6.70 (d, J = 8.4 Hz, 1H, 3,4-di OH phenyl C_5-H), 6.76 (s, 1H, 3,4-di OH phenyl C_2-H), 7.33 (t, J = 7.2 Hz, 1H, 2-Cl phenyl C_4-H), 7.38 (t, J = 7.2 Hz, 1H, 2-Cl phenyl C_5-H), 7.46 (d, J = 8.0 Hz, 1H, 2-Cl phenyl C_3-H), 7.64 (d, J = 7.2 Hz, 1H, 2-Cl phenyl C_6-H). ^{13}C NMR (CD_3OD, 125 MHz) 22.2 (C_6), 28.0 (C_5), 37.7 (C_7), 59.3 (C_9), 109.8 (C_{8a}), 115.5 (3,4-di OH phenyl C_5), 116.2 (3,4-di OH phenyl C_2), 120.0 (3,4-di OH phenyl C_6), 128.0 (2-Cl phenyl C_5), 131.5 (2-Cl phenyl C_6), 131.8 (2-Cl phenyl C_3), 132.7 (2-Cl phenyl C_4), 134.2 (3,4-di OH phenyl C_1), 134.3 (2-Cl phenyl C_2), 146.3 (3,4-di OH phenyl C_4), 146.4 (3,4-di OH phenyl C_3), 148.7 (C_{5a}), 154.5 (CN_2N_4), 160.1 (CN_1N_3), 197.3 (CO).

4.1.30. 2-(2-Chlorophenyl)-9-(4-morpholinophenyl)-5,6,7,9-tetrahydro-[1,2,4]triazolo[5,1-b] quinazolin-8(4H)-one (**9d**)

Yield: 35.8 %, yellowish powder, m.p. 284-286°C. LR-ESI: 460.2 [M-H]$^-$. HR-ESI *m/z* calcd for $C_{25}H_{23}ClN_5O_2$ [M-H]$^-$ 460.1540, found 460.1543. ^{1}H NMR (CD_3OD, 400 MHz) 2.07 (m, 2H, C_6-H), 2.41 (m, 2H, C_5-H), 2.75 (m, 2H, C_7-H), 3.09 (t, J = 5.2 Hz, 4H, morpholino N$\underline{CH_2}$), 3.78 (t, J = 4.8 Hz, 4H, morpholino O$\underline{CH_2}$), 6.36 (s, 1H, C_9-H), 6.88 (d, J = 8.8 Hz, 2H, phenyl $C_{3,5}$-H), 7.20 (d, J = 8.8 Hz, 2H, phenyl $C_{2,6}$-H), 7.33 (dt, J = 7.2 Hz, J = 1.6 Hz, 1H, 2-Cl phenyl C_4-H), 7.40 (dt, J = 8.0 Hz, J = 2.0

Hz, 1H, 2-Cl phenyl C_5-H), 7.46 (dd, *J* = 7.6 Hz, *J* = 1.2 Hz, 1H, 2-Cl phenyl C_3-H), 7.64 (dd, *J* = 7.6 Hz, *J* = 2.0 Hz, 1H, 2-Cl phenyl C_6-H). ^{13}C NMR (CD_3OD, 125 MHz) 22.2 (C_6), 28.0 (C_5), 37.7 (C_7), 50.7 (2C, morpholino N$\underline{CH_2}$), 59.3 (C_9), 68.1 (2C, morpholino O$\underline{CH_2}$), 109.7 (C_{8a}), 116.8 (2C, phenyl $C_{3,5}$), 128.0 (2-Cl phenyl C_5), 129.2 (2C, phenyl $C_{2,6}$), 131.5 (phenyl C_1), 131.6 (2-Cl phenyl C_6), 131.8 (2-Cl phenyl C_3), 132.6 (2-Cl phenyl C_4), 134.0 (2-Cl phenyl C_2), 134.3 (2-Cl phenyl C_1), 148.8 (C_{5a}), 152.8 (phenyl C_4), 154.5 (CN_2N_4), 160.2 (CN_1N_3), 197.2 (CO).

4.1.31. N-(4-(2-(2-Chlorophenyl)-8-oxo-4,5,6,7,8,9-hexahydro-[1,2,4]triazolo[5,1-b]quinazolin-9-yl) phenyl)acetamide (**9e**)

Yield: 55.8 %, yellowish powder, m.p. 290-291°C. LR-ESI: 432.2 [M-H]$^-$. HR-ESI *m*/*z* calcd for $C_{23}H_{19}ClN_5O_2$ [M-H]$^-$ 432.1233, found 432.1237. ^{1}H NMR (CD_3OD, 400 MHz) 2.08 (m, 2H, C_6-H), 2.09 (s, 3H, AcNH), 2.40 (m, 2H, C_5-H), 2.75 (m, 2H, C_7-H), 6.39 (s, 1H, C_9-H), 7.26 (d, *J* = 8.8 Hz, 2H, 4-AcNH phenyl $C_{2,6}$-H), 7.33 (dt, *J* = 7.6 Hz, *J* = 1.6 Hz, 1H, 2-Cl phenyl C_4-H), 7.38 (dt, *J* = 7.2 Hz, *J* = 2.0 Hz, 1H, 2-Cl phenyl C_5-H), 7.48 (d, *J* = 8.8 Hz, 2H, 4-AcNH phenyl $C_{3,5}$-H), 7.64 (dd, *J* = 7.6 Hz, *J* = 2.0 Hz, 1H, 2-Cl phenyl C_3-H), 7.78 (d, *J* = 8.4 Hz, 1H, 2-Cl phenyl C_6-H). ^{13}C NMR (CD_3OD, 100 MHz) 22.2 (C_6), 24.1 (AcNH), 28.0 (C_5), 37.7 (C_7), 59.5 (C_9), 109.4 (C_{8a}), 125.9 (2C, 4-AcNH phenyl $C_{3,5}$), 128.5 (2-Cl phenyl C_5), 128.9 (2C, 4-AcNH phenyl $C_{2,6}$), 129.8 (2-Cl phenyl C_6), 130.8 (2-Cl phenyl C_3), 131.3 (2-Cl phenyl C_4), 132.8 (2-Cl phenyl C_2), 133.0 (4-AcNH phenyl C_1), 134.3 (4-AcNH phenyl C_4), 139.9 (2-Cl phenyl C_1), 151.0 (C_{5a}), 154.9 (CN_2N_4), 160.4 (CN_1N_3), 168.6 ($CH_3\underline{CO}$), 197.2 (CO).

4.1.32. 2-(2-Chlorophenyl)-9-(4-ethylphenyl)-5,6,7,9-tetrahydro-[1,2,4]triazolo[5,1-b]quinazolin- 8(4H)-one (**9f**)

Yield: 45.7 %, yellowish powder. LR-ESI: 403.3 [M-H]$^-$. HR-ESI *m*/*z* calcd for $C_{23}H_{20}ClN_4O$ [M-H]$^-$ 403.1326, found 403.1324. ^{1}H NMR (CD_3OD, 400 MHz) 1.17 (t, *J* = 7.6 Hz, 3H, $CH_2\underline{CH_3}$), 2.04 (m, 2H, C_6-H), 2.39 (m, 2H, C_5-H), 2.58 (q, *J* = 7.6 Hz, 2H, $\underline{CH_2}CH_3$), 2.76 (m, 2H, C_7-H), 6.39 (s, 1H, C_9-H), 7.12 (d, *J* = 8.0 Hz, 2H, 4-Et phenyl $C_{3,5}$-H), 7.21 (d, *J* = 8.0 Hz, 2H, 4-Et phenyl $C_{2,6}$-H), 7.32 (dt, *J* = 7.6 Hz, *J* = 1.6 Hz, 1H, 2-Cl phenyl C_4-H), 7.37 (dt, *J* = 8.0 Hz, *J* = 2.0 Hz, 1H, 2-Cl phenyl C_5-H), 7.46 (dd, *J* = 8.0 Hz, *J* = 1.6 Hz, 1H, 2-Cl phenyl C_3-H), 7.63 (dd, *J* = 7.6 Hz, *J* = 2.0 Hz, 1H, 2-Cl phenyl C_6-H). ^{13}C NMR (CD_3OD, 125 MHz) 16.2 ($CH_2\underline{CH_3}$), 22.2 (C_6), 28.0 (C_5), 29.6 ($\underline{CH_2}CH_3$), 37.7 (C_7), 59.6 (C_9), 109.6 (C_{8a}), 128.0 (2-Cl phenyl C_5), 128.4 (2C, 4-Et phenyl $C_{3,5}$), 129.1 (2C, 4-Et phenyl $C_{2,6}$), 131.4 (2-Cl phenyl C_2), 131.5 (2-Cl phenyl C_6), 131.8 (2-Cl phenyl C_3), 132.6 (2-Cl phenyl C_4), 134.2 (4-Et phenyl C_1), 139.9 (2-Cl phenyl C_1), 145.7 (4-Et phenyl C_4), 148.9 (C_{5a}), 154.8 (CN_2N_4), 160.3 (CN_1N_3), 197.2 (CO).

4.1.33. 2-(2-Chlorophenyl)-9-(4-(methylthio)phenyl)-5,6,7,9-tetrahydro-[1,2,4]triazolo[5,1-b] quinazolin-8(4H)-one (**9g**)

Yield: 49.7 %, yellowish powder, m.p. 255-256°C. LR-ESI: 421.1 $[M-H]^-$. HR-ESI *m/z* calcd for $C_{22}H_{18}ClN_4OS$ $[M-H]^-$ 421.0890, found 421.0897. ^{1}H NMR (CD_3OD, 400 MHz) 2.06 (m, 2H, C_6-H), 2.41 (m, 2H, C_5-H), 2.43 (s, 3H, $\underline{CH_3}S$), 2.76 (m, 2H, C_7-H), 6.39 (s, 1H, C_9-H), 7.19 (d, J = 8.8 Hz, 2H, 4-CH_3S phenyl $C_{2,6}$-H), 7.24 (d, J = 8.4 Hz, 2H, 4-CH_3S phenyl $C_{3,5}$-H), 7.33 (dt, J = 7.6 Hz, J = 1.6 Hz, 1H, 2-Cl phenyl C_4-H), 7.38 (dt, J = 8.0 Hz, J = 2.0 Hz, 1H, 2-Cl phenyl C_5-H), 7.46 (dd, J = 8.0 Hz, J = 1.6 Hz, 1H, 2-Cl phenyl C_3-H), 7.64 (dd, J = 7.6 Hz, J = 2.0 Hz, 1H, 2-Cl phenyl C_6-H). ^{13}C NMR (CD_3OD, 125 MHz) 15.6 ($\underline{CH_3}S$), 22.2 (C_6), 28.0 (C_5), 37.7 (C_7), 59.5 (C_9), 109.3 (C_{8a}), 127.5 (2C, 4-CH_3S phenyl $C_{3,5}$), 128.0 (2-Cl phenyl C_5), 128.9 (2C, 4-CH_3S phenyl $C_{2,6}$), 131.5 (2-Cl phenyl C_2), 131.6 (2-Cl phenyl C_6), 131.8 (2-Cl phenyl C_3), 132.6 (2-Cl phenyl C_4), 134.3 (4-CH_3S phenyl C_1), 139.3 (2-Cl phenyl C_1), 140.3 (4-CH_3S phenyl C_4), 148.9 (C_{5a}), 155.0 (CN_2N_4), 160.4 (CN_1N_3), 197.1 (CO).

4.1.34. 2-(2-Chlorophenyl)-9-(4-(pyrrolidin-1-yl)phenyl)-5,6,7,9-tetrahydro-[1,2,4]triazolo[5,1-b] quinazolin-8(4H)-one (**9h**)

Yield: 39.0 %, yellowish powder, m.p. 280-282°C. LR-ESI: 444.2 $[M-H]^-$. HR-ESI *m/z* calcd for $C_{25}H_{23}ClN_5O$ $[M-H]^-$ 444.1591, found 444.1593. ^{1}H NMR (CD_3OD, 400 MHz) 1.98 (m, 4H, pyrrolidinyl $C_{3,4}$-H), 2.03 (m, 1H, C_6-H), 2.20 (m, 1H, C_6-H), 2.40 (m, 2H, C_5-H), 2.77 (m, 2H, C_7-H), 3.22 (m, 4H, pyrrolidinyl $C_{2,5}$-H), 6.31 (s, 1H, C_9-H), 6.48 (d, J = 8.4 Hz, 2H, 4-pyrrolidinyl phenyl $C_{3,5}$-H), 7.12 (d, J = 8.8 Hz, 2H, 4-pyrrolidinyl phenyl $C_{2,6}$-H), 7.33 (dt, J = 7.6 Hz, J = 1.6 Hz, 1H, 2-Cl phenyl C_4-H), 7.38 (dt, J = 7.2 Hz, J = 1.6 Hz, 1H, 2-Cl phenyl C_5-H), 7.47 (dd, J = 8.0 Hz, J = 1.6 Hz, 1H, 2-Cl phenyl C_3-H), 7.63 (dd, J = 7.6 Hz, J = 2.0 Hz, 1H, 2-Cl phenyl C_6-H). ^{13}C NMR (CD_3OD, 125 MHz) 22.3 (C_6), 26.5 (2C, pyrrolidinyl $C_{3,4}$), 28.0 (C_5), 37.7 (C_7), 58.5 (2C, pyrrolidinyl $C_{2,5}$), 59.5 (C_9), 110.1 (C_{8a}), 112.7 (2C, 4-pyrrolidinyl phenyl $C_{3,5}$), 128.0 (2-Cl phenyl C_5), 128.1 (2-Cl phenyl C_6), 129.1 (2C, 4-pyrrolidinyl phenyl $C_{2,6}$), 129.3 (4-pyrrolidinyl phenyl C_1), 131.5 (2-Cl phenyl C_2), 131.9 (2-Cl phenyl C_3), 132.7 (2-Cl phenyl C_4), 140.0 (2-Cl phenyl C_1), 148.8 (C_{5a}), 149.6 (4-pyrrolidinyl phenyl C_4), 154.9 (CN_2N_4), 160.1 (CN_1N_3), 197.4 (CO).

4.1.35. 2-(2-Chlorophenyl)-9-(4-mercaptophenyl)-5,6,7,9-tetrahydro-[1,2,4]triazolo [5,1-b] quinazolin-8(4H)-one (**9i**)

LR-ESI: 409.1 $[M+H]^+$. HR-ESI *m/z* calcd for $C_{21}H_{18}ClN_4OS$ $[M+H]^+$ 409.0890, found 409.0895. ^1H NMR (CD_3OD, 400 MHz) 2.09 (m, 2H, C_6-H), 2.40 (m, 2H, C_5-H), 2.76 (m, 2H, C_7-H), 6.34 (s, 1H, C_9-H), 7.04 (d, J = 8.8 Hz, 2H, 4-SH phenyl $C_{2,6}$-H), 7.24 (d, J = 8.4 Hz, 2H, 4-SH phenyl $C_{3,5}$-H), 7.33 (dt, J = 1.2 Hz, J = 7.6 Hz, 1H, 2-Cl phenyl C_5-H), 7.38 (dt, J = 1.6 Hz, J = 7.6 Hz, 1H, 2-Cl phenyl C_4-H), 7.47 (d, J = 8.0 Hz, 1H, 2-Cl phenyl C_3-H), 7.63 (dd, J = 2.0 Hz, J = 7.6 Hz, 1H, 2-Cl phenyl C_6-H).

4.1.36. 2-(2-Chlorophenyl)-9-(4-hydroxyphenyl)-6,6-dimethyl-5,6,7,9-tetrahydro-[1,2,4]triazolo [5,1-b]quinazolin-8(4H)-one (**11a**)

Yield: 57.2%, yellowish powder, m.p. 228-229°C. LR-ESI: 419.2 $[M-H]^-$. HR-ESI *m/z* calcd for $C_{23}H_{20}ClN_4O_2$ $[M-H]^-$ 419.1275, found 419.1278. ^1H NMR (CD_3OD, 400 MHz) 1.06 (s, 3H, C_6-CH_3), 1.14 (s, 3H, C_6-CH_3), 2.21 (d, J = 16.4 Hz, 1H, C_5-H), 2.34 (d, J = 16.4 Hz, 1H, C_5-H), 2.59 (d, J = 17.2 Hz, 1H, C_7-H), 2.65 (d, J = 16.8 Hz, 1H, C_7-H), 6.31 (s, 1H, C_9-H), 6.71 (d, J = 8.0 Hz, 2H, 4-OH phenyl $C_{3,5}$-H), 7.13 (d, J = 8.0 Hz, 2H, 4-OH phenyl $C_{2,6}$-H), 7.34 (t, J = 7.6 Hz, 1H, 2-Cl phenyl C_4-H), 7.39 (t, J = 7.6 Hz, 1H, 2-Cl phenyl C_5-H), 7.47 (d, J = 8.0 Hz, 1H, 2-Cl phenyl C_3-H), 7.63 (d, J = 7.2 Hz, 1H, 2-Cl phenyl C_6-H). ^{13}C NMR (CD_3OD, 125 MHz) 27.6 (C_6-CH_3), 29.3 (C_6-CH_3), 33.7 (C_6), 41.3 (C_5), 51.3 (C_7), 59.6 (C_9), 108.9 (C_{8a}), 116.3 (2C, 4-OH phenyl $C_{3,5}$), 128.0 (2-Cl phenyl C_5), 129.6 (2C, 4-OH phenyl $C_{2,6}$), 131.5 (2-Cl phenyl C_6), 131.8 (2-Cl phenyl C_3), 132.7 (2-Cl phenyl C_4), 132.9 (C_{5a}), 133.6 (4-OH phenyl C_1), 134.3 (2-Cl phenyl C_2), 148.9 (2-Cl phenyl C_1), 152.6 (CN_2N_4), 158.6 (4-OH phenyl C_4), 160.3 (CN_1N_3), 196.9 (CO).

4.1.37. 2-(2-Chlorophenyl)-9-(4-hydroxyphenyl)-5,5-dimethyl-5,6,7,9-tetrahydro-[1,2,4]triazolo [5,1-b]quinazolin-8(4H)-one (**11b**)

Yield: 67.2%, white powder, m.p. 227-229°C. LR-ESI: 419.1 $[M-H]^-$. HR-ESI *m/z* calcd for $C_{23}H_{20}ClN_4O_2$ $[M-H]^-$ 419.1275, found 419.1279. ^1H NMR (CD_3OD, 400 MHz) 1.02 (s, 3H, C_5-CH_3), 1.11 (s, 3H, C_5-CH_3), 1.91 (m, 2H, C_6-H), 2.74 (m, 2H, C_7-H), 6.29 (s, 1H, C_9-H), 6.70 (d, J = 8.4 Hz, 2H, 4-OH phenyl $C_{3,5}$-H), 7.12 (d, J = 8.4 Hz, 2H, 4-OH phenyl $C_{2,6}$-H), 7.32 (t, J = 7.6 Hz, 1H, 2-Cl phenyl C_3-H), 7.37 (t, J = 8.0 Hz, 1H, 2-Cl phenyl C_5-H), 7.46 (d, J = 8.0 Hz, 1H, 2-Cl phenyl C_3-H), 7.62 (d, J = 7.2 Hz, 1H, 2-Cl phenyl C_6-H). ^{13}C NMR (CD_3OD, 125 MHz) 24.8 (C_5-CH_3), 25.3 (C_5-CH_3), 35.7 (2C, $C_{6,7}$), 41.3 (C_5), 59.6 (C_9), 108.2 (C_{8a}), 116.3 (2C, 4-OH phenyl $C_{3,5}$), 128.0 (2-Cl phenyl C_5), 129.6 (2C, 4-OH phenyl $C_{2,6}$), 131.5 (2-Cl phenyl C_6), 131.8 (2-Cl phenyl C_3), 132.6 (2-Cl phenyl C_4), 133.6 (4-OH phenyl C_1), 134.3 (2-Cl phenyl C_2), 148.7 (2-Cl phenyl C_1), 152.6 (CN_2N_4), 158.5 (4-OH phenyl C_4), 160.2

(CN_1N_3), 172.4 (C_{5a}), 202.1 (CO).

4.1.38. 2-(2-Chlorophenyl)-9-(4-hydroxyphenyl)-7,9-dihydro-4H-pyrano[3,4-d][1,2,4]triazolo[1,5-a] pyrimidin-8(5H)-one (**11c**)

Yield: 58.8%, yellowish powder, m.p. 208-209°C. LR-ESI: 393.1 $[M-H]^-$. HR-ESI *m/z* calcd for $C_{20}H_{14}ClN_4O_3$ $[M-H]^-$ 393.0754, found 393.0757. ^1H NMR (CD_3OD, 400 MHz) 4.13 (s, 2H, C_5-H), 4.61 (d, J = 16.0 Hz, 1H, C_7-H), 4.69 (d, J = 16.4 Hz, 1H, C_7-H), 6.40 (s, 1H, C_9-H), 6.73 (d, J = 7.6 Hz, 2H, 4-OH phenyl $C_{3,5}$-H), 7.16 (d, J = 7.6 Hz, 2H, 4-OH phenyl $C_{2,6}$-H), 7.33 (t, J = 7.2 Hz, 1H, 2-Cl phenyl C_4-H), 7.38 (t, J = 7.6 Hz, 1H, 2-Cl phenyl C_5-H), 7.46 (d, J = 8.0 Hz, 1H, 2-Cl phenyl C_3-H), 7.65 (d, J = 7.2 Hz, 1H, 2-Cl phenyl C_6-H). ^{13}C NMR (CD_3OD, 125 MHz) 58.8 (C_9), 65.0 (C_7), 72.6 (C_5), 107.1 (C_{8a}), 116.4 (2C, 4-OH phenyl $C_{3,5}$), 128.0 (2-Cl phenyl C_5), 129.6 (2C, 4-OH phenyl $C_{2,6}$), 131.4 (4-OH phenyl C_1), 131.5 (2-Cl phenyl C_6), 131.8 (2-Cl phenyl C_3), 132.6 (2-Cl phenyl C_4), 132.8 (2-Cl phenyl C_2), 134.2 (2-Cl phenyl C_1), 148.3 (CN_2N_4), 152.4 (C_{5a}), 158.8 (4-OH phenyl C_4), 160.3 (CN_1N_3), 192.6 (CO).

4.1.39. 2-(2-Chlorophenyl)-9-(4-hydroxyphenyl)-5,9-dihydro-4H-thiopyrano[3,4-d][1,2,4]triazolo [1,5-a]pyrimidin-8(7H)-one (**11d**)

Yield: 58.6%, yellowish powder, m.p. 211-213°C. LR-ESI: 409.1 $[M-H]^-$. HR-ESI *m/z* calcd for $C_{20}H_{14}ClN_4O_2S$ $[M-H]^-$ 409.0526, found 409.0531. ^1H NMR (CD_3OD, 500 MHz) 3.18 (dd, J = 2.0 Hz, J = 16.0 Hz, 1H, C_5-H), 3.56 (dd, J = 2.0 Hz, J = 16.5 Hz, 1H, C_5-H), 3.62 (dd, J = 1.5 Hz, J = 17.0 Hz, 1H, C_7-H), 3.95 (d, J = 17.0 Hz, 1H, C_7-H), 6.39 (s, 1H, C_9-H), 6.72 (d, J = 8.5 Hz, 2H, 4-OH phenyl $C_{3,5}$-H), 7.18 (d, J = 8.5 Hz, 2H, 4-OH phenyl $C_{2,6}$-H), 7.34 (dt, J = 1.5 Hz, J = 7.5 Hz, 1H, 2-Cl phenyl C_4-H), 7.39 (dt, J = 1.5 Hz, J = 7.5 Hz, 1H, 2-Cl phenyl C_5-H), 7.47 (dd, J = 1.5 Hz, J = 8.0 Hz, 1H, 2-Cl phenyl C_3-H), 7.64 (dd, J = 1.5 Hz, J = 7.5 Hz, 1H, 2-Cl phenyl C_6-H). ^{13}C NMR (CD_3OD, 125 MHz) 27.6 (C_5), 35.4 (C_7), 59.3 (C_9), 108.8 (C_{8a}), 116.3 (2C, 4-OH phenyl $C_{3,5}$), 128.0 (2-Cl phenyl C_5), 129.6 (2C, 4-OH phenyl $C_{2,6}$), 131.4 (4-OH phenyl C_1), 131.5 (2-Cl phenyl C_6), 131.8 (2-Cl phenyl C_3), 132.7 (2-Cl phenyl C_4), 133.2 (2-Cl phenyl C_2), 134.3 (2-Cl phenyl C_1), 148.3 (C_{5a}), 152.1 (CN_2N_4), 158.7 (4-OH phenyl C_4), 160.3 (CN_1N_3), 191.6 (CO).

4.1.40. 9-(4-Hydroxyphenyl)-5,6,7,9-tetrahydro-[1,2,4]triazolo[5,1-b]quinazolin-8(4H)-one (**13a**)

Yield: 69.5%, white powder, m.p. 230-231°C. LR-ESI: 281.2 (M-1). HR-ESI *m/z* calcd for $C_{15}H_{13}N_4O_2$ $[M-H]^-$ 281.1039, found 281.1042. ^1H NMR (DMSO-d_6, 400 MHz) 1.94 (m, 2H, C_6-H), 2.25 (m, 2H, C_5-H), 2.65 (m, 2H, C_7-H), 6.11 (s, 1H, C_9-H), 6.64

(d, J = 7.6 Hz, 2H, 4-OH phenyl $C_{3,5}$-H), 6.99 (d, J = 7.6 Hz, 2H, 4-OH phenyl $C_{2,6}$-H), 7.65 (s, 1H, C_2-H), 9.36 (s, OH), 11.0 (s, NH). ^{13}C NMR (DMSO-d_6, 125 MHz) 20.7 (C_6), 26.4 (C_5), 36.4 (C_7), 57.1 (C_9), 106.8 (C_{8a}), 114.9 (2C, 4-OH phenyl $C_{3,5}$), 128.1 (2C, 4-OH phenyl $C_{2,6}$), 132.1 (4-OH phenyl C_1), 146.7 (C_{5a}), 149.8 (C_2), 152.3 (CN_2N_4), 156.9 (4-OH phenyl C_4), 193.2 (CO).

4.1.41. 9-(4-Hydroxyphenyl)-5,6,7,9-tetrahydrotetrazolo[5,1-b]quinazolin-8(4H)-one (**13b**)

Yield: 75.8%, yellowish powder. LR-ESI: 282.1 [M-H]$^-$. HR-ESI m/z calcd for $C_{14}H_{12}N_5O_2$ [M-H]$^-$ 282.0991, found 282.0993. ^{1}H NMR (CD_3OD, 400 MHz) 2.09 (m, 2H, C_6-H), 2.40 (m, 2H, C_5-H), 2.78 (m, 2H, C_7-H), 6.58 (s, 1H, C_9-H), 6.72 (d, J = 8.0 Hz, 2H, 4-OH phenyl $C_{3,5}$-H), 7.13 (d, J = 8.0 Hz, 2H, 4-OH phenyl $C_{2,6}$-H). ^{13}C NMR (CD_3OD, 125 MHz) 22.2 (C_6), 28.3 (C_5), 37.7 (C_7), 58.9 (C_9), 109.2 (C_{8a}), 116.5 (2C, 4-OH phenyl $C_{3,5}$), 129.7 (2C, 4-OH phenyl $C_{2,6}$), 132.7 (4-OH phenyl C_1), 150.3 (C_{5a}), 155.5 (4-OH phenyl C_4), 159.0 (tetrazole), 196.9 (CO).

4.1.42. 2-(2-Chlorophenyl)-9-(4-hydroxyphenyl)-5,6,7,9-tetrahydropyrazolo[5,1-b]quinazolin-8(4H)- one (**13c**)

Yield: 75.0%, yellowish powder, m.p. 256-258°C. LR-ESI: 390.1 [M-H]$^-$. HR-ESI m/z calcd for $C_{22}H_{17}ClN_3O_2$ [M-H]$^-$ 390.1009, found 390.1012. ^{1}H NMR (CD_3OD, 400 MHz) 2.02 (m, 2H, C_6-H), 2.35 (m, 2H, C_5-H), 2.70 (m, 2H, C_7-H), 6.21 (s, 1H, C_9-H), 6.32 (s, 1H, C_3-H), 6.66 (d, J = 7.6 Hz, 2H, 4-OH phenyl $C_{3,5}$-H), 7.07 (d, J = 7.6 Hz, 2H, 4-OH phenyl $C_{2,6}$-H), 7.28 (m, 2H, 2-Cl phenyl $C_{4,5}$-H), 7.43 (m, 1H, 2-Cl phenyl C_3-H), 7.56 (m, 1H, 2-Cl phenyl C_6-H). ^{13}C NMR (CD_3OD, 125 MHz) 22.3 (C_6), 28.1 (C_5), 37.6 (C_7), 58.7 (C_9), 91.3 (C_3), 108.8 (C_{8a}), 116.0 (2C, 4-OH phenyl $C_{3,5}$), 128.1 (2-Cl phenyl C_6), 129.2 (2C, 4-OH phenyl $C_{2,6}$), 130.6 (2-Cl phenyl C_4), 131.3 (2-Cl phenyl C_5), 131.8 (CN_2N_3), 132.0 (2-Cl phenyl C_3), 133.6 (2-Cl phenyl C_1), 135.1 (4-OH phenyl C_1), 139.2 (2-Cl phenyl C_2), 150.9 (C_{5a}), 153.9 (C_2), 158.0 (4-OH phenyl C_4), 196.9 (CO).

4.1.43. 2-(2-Bromophenyl)-9-(4-hydroxyphenyl)-7,9-dihydro-4H-thiopyrano[3,4-d][1,2,4]triazolo[1,5-a]pyrimidin-8(5H)-one (**14a**)

Yield: 49.5%, yellowish powder, m.p. 295-296°C. LR-ESI: 455.0 [M+H]$^+$. HR-ESI m/z calcd for $C_{20}H_{16}BrN_4O_2S$ [M+H]$^+$ 455.0172, found 455.0162. ^{1}H NMR (CD_3OD, 400 MHz) 3.16 (d, J = 16.0 Hz, 1H, C_5-H), 3.54 (d, J = 17.2 Hz, 2H, $C_{5,7}$-H), 3.89 (d, J = 17.2 Hz, 1H, C_7-H), 6.38 (s, 1H, C_9-H), 6.71 (d, J = 8.8 Hz, 2H, 4-OH phenyl $C_{3,5}$-H), 7.18 (d, J = 8.8 Hz, 2H, 4-OH phenyl $C_{2,6}$-H), 7.30 (t, J = 8.0 Hz, 1H, 2-Br phenyl C_4-

H), 7.38 (t, J = 7.6 Hz, 1H, 2-Br phenyl C_5-H), 7.57 (dd, J = 1.6 Hz, J = 7.6 Hz, 1H, 2-Br phenyl C_3-H), 7.66 (d, J = 8.4 Hz, 1H, 2-Br phenyl C_6-H). ^{13}C NMR (CD_3OD, 125 MHz) 27.5 (C_5), 35.4 (C_7), 59.3 (C_9), 108.9 (C_{8a}), 116.3 (2C, 4-OH phenyl $C_{3,5}$), 123.4 (2-Br phenyl C_2), 128.5 (2-Br phenyl C_5), 129.7 (2C, 4-OH phenyl $C_{2,6}$), 132.0 (2-Br phenyl C_6), 132.8 (2-Br phenyl C_4), 133.2 (4-OH phenyl C_1), 133.6 (C_{5a}), 134.8 (2-Br phenyl C_3), 148.2 (2-Br phenyl C_1), 151.9 (CN_2N_4), 158.7 (4-OH phenyl C_4), 161.3 (CN_1N_3), 191.5 (CO).

4.1.44. 9-(4-Hydroxyphenyl)-2-(2-iodophenyl)-7,9-dihydro-4H-thiopyrano[3,4-d][1,2,4]triazolo[1,5-a]pyrimidin-8(5H)-one **(14b)**

Yield: 50.5%, yellowish powder, m.p. >300°C. LR-ESI: 501.1 (M-1). HR-ESI *m/z* calcd for $C_{20}H_{14}IN_4O_2S$ $[M-H]^-$ 500.9882, found 500.9885. ^{1}H NMR (CD_3OD, 400 MHz) 3.15 (dd, J = 2.0 Hz, J = 16.0 Hz, 1H, C_5-H), 3.53 (m, 2H, $C_{5,7}$-H), 3.87 (dd, J = 2.0 Hz, J = 17.2 Hz, 1H, C_7-H), 6.36 (s, 1H, C_9-H), 6.71 (d, J = 8.8 Hz, 2H, 4-OH phenyl $C_{3,5}$-H), 7.11 (dt, J = 1.6 Hz, J = 7.6 Hz, 1H, 2-I phenyl C_5-H), 7.18 (d, J = 8.8 Hz, 2H, 4-OH phenyl $C_{2,6}$-H), 7.39 (dt, J = 1.2 Hz, J = 7.6 Hz, 1H, 2-I phenyl C_4-H), 7.48 (dd, J = 1.6 Hz, J = 7.6 Hz, 1H, 2-I phenyl C_6-H), 7.93 (d, J = 8.0 Hz, 1H, 2-I phenyl C_3-H). ^{13}C NMR (CD_3OD, 125 MHz) 27.6 (C_5), 35.4 (C_7), 59.3 (C_9), 97.4 (2-I phenyl C_2), 108.8 (C_{8a}), 116.3 (2C, 4-OH phenyl $C_{3,5}$), 127.4 (2-I phenyl C_5), 129.2 (2-I phenyl C_6), 129.7 (2C, 4-OH phenyl $C_{2,6}$), 132.0 (2-I phenyl C_4), 133.2 (4-OH phenyl C_1), 137.6 (C_{5a}), 141.3 (2-I phenyl C_3), 148.2 (2-I phenyl C_1), 152.0 (CN_2N_4), 158.6 (4-OH phenyl C_4), 163.0 (CN_1N_3), 191.5 (CO).

4.1.45. 9-(4-Hydroxyphenyl)-2-(2-(trifluoromethyl)phenyl)-7,9-dihydro-4H-thiopyrano[3,4-d][1,2,4] triazolo[1,5-a]pyrimidin-8(5H)-one **(14c)**

Yield: 40.9%, yellowish powder, m.p. 240-241°C. LR-ESI: 443.2 (M-1). HR-ESI *m/z* calcd for $C_{21}H_{14}F_3N_4O_2S$ $[M-H]^-$ 443.0790, found 443.0797. ^{1}H NMR (CD_3OD, 400 MHz) 3.18 (dd, J = 16.4 Hz, J = 2.4 Hz, 1H, C_5-H), 3.57 (dd, J = 16.0 Hz, J = 2.0 Hz, 1H, C_5-H), 3.60 (dd, J = 16.8 Hz, J = 2.0 Hz, 1H, C_7-H), 3.94 (d, J = 16.8 Hz, 1H, C_7-H), 6.38 (s, 1H, C_9-H), 6.71 (d, J = 8.8 Hz, 2H, 4-OH phenyl $C_{3,5}$-H), 7.16 (d, J = 8.8 Hz, 2H, 4-OH phenyl $C_{2,6}$-H), 7.64 (m, 3H, 2-CF_3 phenyl $C_{3,4,5}$-H), 7.78 (d, J = 7.6 Hz, 1H, 2-CF_3 phenyl C_6-H). ^{13}C NMR (CD_3OD, 125 MHz) 27.5 (C_5), 35.4 (C_7), 59.3 (C_9), 108.9 (C_{8a}), 116.3 (2C, 4-OH phenyl $C_{3,5}$), 127.6 (CF_3), 127.7 (2-CF_3 phenyl C_3), 129.6 (2C, 4-OH phenyl $C_{2,6}$), 130.5 (2-CF_3 phenyl C_2), 131.0 (2-CF_3 phenyl C_4), 131.5 (C_{5a}), 133.0 (2-CF_3 phenyl C_6), 133.1 (2-CF_3 phenyl C_5), 133.2 (4-OH phenyl C_1), 148.4 (2-CF_3 phenyl C_1), 152.1 (CN_2N_4), 158.7 (4-OH phenyl C_4), 160.6 (CN_1N_3), 191.5 (CO).

*4.2. Chiral resolution of compound **7a***

The enantiomers of compound **7a** (1.57 g) were resolved by CHIRALPAK IC (IC00CD-NA012) column (0.46 cm × 15 cm) on Shimadzu LC-20AT HPLC eluting with dichloromethane/ethanol [90/10 (v/v)] with a flow rate of 1.0 mL/min at 35°C under the wavelength of UV 254 nm.. Two peaks were separately collected at the *tR* = 2.090 min (isomer 1) and *tR* = 2.409 min (isomer 2) and the enantiomeric excess (*e.e.*) value of each product is determined by HPLC as >98%. Two isomers were thus obtained as light yellowish powder (isomer 1: 0.71 g; isomer 2: 0.71 g). The absolute configuration of isomer 1 was determined by X-ray diffraction as 9-(*R*)-**7a**. Specific optical rotation was also detected for these two isomers. Isomer 1: 9-(*R*)-**7a**, $[\alpha]^{D}_{20}$ -110° (c 0.1 in methanol); Isomer 2: 9-(*S*)-**7a**, $[\alpha]^{D}_{20}$ +107° (c 0.1 in methanol).

*4.3. Chiral resolution of compound **14b***

The enantiomers of compound **14b** (0.0705 *g*) were resolved by CHIRALPAK IC column (0.46 cm × 15 cm) on Shimadzu LC-2010 HPLC eluting with ethanol with a flow rate of 1.0 mL/min at 25°C under the wavelength of UV 210 nm. Two peaks were separately collected at the *tR* = 4.568 min (isomer 1) and *tR* = 5.981 min (isomer 2) and the enantiomeric excess (*e.e.*) value of each product is determined by HPLC as >99%. Two isomers were thus obtained as white powder (isomer 1: 0.0309 g; isomer 2: 0.0255 g). Specific optical rotation was detected for these two isomers. Isomer 1: 9-(*R*)-**14b**, $[\alpha]^{D}_{20}$ -22° (c 0.1 in methanol); Isomer 2: 9-(*S*)-**14b**, $[\alpha]^{D}_{20}$ +22° (c 0.1 in methanol).

*4.4. X-ray structure determination of 9-(R)-7**a** (isomer 1)*

Diffraction data were collected on a Bruker D8 VENTURE single-crystal diffractometer using a graphite-monochromated MoKα radiation (0.71073Å) at 193 K in the ω-2θ scan mode. In this case, an empirical absorption correction by SADABS was applied to the intensity data. The structure was solved by direct methods and refined by full-matrix least-squares on F^2 methods using the SHELXTL crystallographic software package. All non-hydrogen atoms were refined anisotropically with hydrogen atoms included in calculated positions (riding model). Crystallographic data for compound 9-(*R*)-**7a** is given in Table S2-7. CCDC2004638 contains the supplementary crystallographic data for compound 9-(*R*)-**7a**, which can be obtained free of charge from The Cambridge Crystallographic Data Centre *via* www.ccdc.cam.ac.uk/data_request/cif.

4.5. Bioassays

4.5.1. Reagents

Human INSL5 (hINSL5), R3/I5 and relaxin-3 were purchased from Phoenix Pharmaceuticals (Burlingame, USA). LANCE Ultra cAMP and AlphaScreen SureFire p-ERK1/2 assay kits were obtained from PerkinElmer (Waltham, MA, USA). Forskolin, 3-isobutyl-1-methylxanthine (IBMX), dimethyl sulfoxide (DMSO) and bovine serum albumin were supplied by Sigma-Aldrich (St. Louis, USA). The methods for plasmid construction, cell culture and assay validation were described in our previous paper [14].

4.5.2. cAMP accumulation assay

For off-target examination, inhibition of forskolin-induced cAMP accumulation by test compounds was carried out in parental CHO cells. For selective agonist effect valuation, compounds were tested for their ability to inhibit cAMP accumulation in CHO-K1 cells stably over-expressing human RXFP4 or human RXFP3. Cells were seeded at a density of 8×10^5 cells/mL and stimulated with different concentrations of individual testing compounds (250, 100, 40, 16, 6.4, 2.56, 1.024 and 0.4096 μM) plus 500 nM forskolin for 40 min at RT in the presence of 500 nM IBMX. Peptides INSL5 and R3I5 were used as positive controls at different concentrations (μM). For cAMP assay on hRXFP1-overexpressing 293T cells, relaxin-3 was used as positive control without forskolin stimulation. Eu-cAMP tracer and ULight-anti-cAMP working solution were then applied followed by incubation for 40 min at RT. Time-resolved fluorescence resonance energy transfer (TR-FRET) signals were read on an EnVision® multimode plate reader (PerkinElmer) with excitation at 320 or 340 nm and emission at 665 nm and 615 nm. Each compound was tested in duplicate and each experiment was performed independently three times. Agonist activity was expressed as % INSL5 in hRXFP4-CHO-K1 cells, % R3/I5 in hRXFP3-CHO-K1 cells or % relaxin-3 in hRXFP1-293T cells. For each ligand-concentration, the value of 665/615 was calculated, and normalized to the corresponding maximum value obtained for INSL5 in hRXFP4-CHO-K1 cells, R3/I5 in hRXFP3-CHO-K1 cells and relaxin-3 in hRXFP1-293T cells. The normalized values were plotted *vs*. ligand concentration using GraphPad PRISM 8 and are expressed as means ± SEM.

4.5.3. Cytotoxicity assay

Cytotoxicity was assessed in hRXFP4-CHO cells using the Cell Counting Kit-8 (CCK-8; Dojindo, Kumamoto, Japan). Cells were seeded into 96-well plates at a density of 30,000 cells/well and incubated overnight, in which different concentrations of compounds were added and incubated for 24 h. CCK-8 solution was then added and incubated for another 1 h. Absorbance values at 450 nm were quantitated on a

SpectraMax M5 plate reader (Molecular Devices). Data were normalized to the vehicle-treated samples (Supplementary Information).

4.5.4. Receptor binding assay

CHO-K1 cells stably expressing human RXFP4 were plated out at the density of 50,000 cells per well per 200 μL in a 96-well ViewPlate with clear bottom and white walls precoated with poly-L-lysine. Competitive binding assay was performed with 5 nM of europium-labeled Eu(A)-R3/I5 in the presence of increasing amounts of test compounds dissolved in DMSO following the protocol described previously [18]. Fluorescence measurement was carried out at an excitation wavelength of 340 nm and an emission wavelength of 614 nm on a Victor Plate Reader (PerkinElmer, Melbourne, Australia). Each concentration point was measured in triplicate, and each experiment was performed independently three times. Data were analyzed using GraphPad PRISM 8 (GraphPad Inc., San Diego, CA) and expressed as means ± SEM.

4.5.5. Statistical analysis

Dose-response data were analyzed with Prism software (GraphPad PRISM 8) using a sigmoidal model with variable slope. Statistical significance was determined using two tailed student's *t*-test, and $P < 0.05$ was considered significant.

4.6. Molecular modelling

Molecular docking for the binding of derivatives to hRXFP4 and hRXFP3 was performed using the LibDock docking protocol in BIOVIA Discovery Studio 2016 (Accelrys).

4.6.1. Preparation of target protein

Homology models of RXFP4 (SWISS-MODEL: Q8TDU9) and RXFP3 (SWISS-MODEL: Q9NSD7), which were modeled on the template of agonist-bound apelin receptor (PDB code: 5VBL), were downloaded from SWISS-MODEL at https://swissmodel.expasy.org/repository/uniprot/. The energy of the system was minimized using CHARMm forcefield.

4.6.2. Preparation of ligands

Ligands were prepared by energy minimization with the top 10 poses to be presented and scored while and keeping the other options in their default values using CHARMm forcefield until RMS gradient of 0.01 was reached.

4.6.3. Molecular docking

Cavity searching was performed to find the hRXFP4 orthosteric binding site constructed by residues L118$^{3.29}$, T176$^{4.60}$, R208$^{5.42}$, F291$^{7.35}$, Q205$^{5.39}$, T266$^{6.55}$, G269$^{6.58}$, V265$^{6.54}$, Q287$^{7.31}$, K273$^{6.62}$, Y284$^{7.28}$, T288$^{7.32}$, L201$^{5.35}$, P196$^{5.30}$, L193, L192, L190 and Y204$^{5.38}$, and the hRXFP3 orthosteric binding site constructed by residues T346$^{6.55}$, Y369$^{7.33}$, L345$^{6.54}$, L365$^{7.29}$, C366$^{7.30}$, S349$^{6.58}$, Y267$^{5.38}$, L264$^{5.35}$, I350$^{6.59}$, K353$^{6.62}$, F262^{ECL2}, W263$^{5.34}$, R250^{ECL2} and F251^{ECL2}. Then the prepared ligand **7a** and **14b** were docked into the binding site using LibDock protocol, with the top 10 poses presented and scored while keeping other options in their default values. LibDock fitness scores of 114.064 (**7a**) and 111.977 (**14b**) for hRXFP4, and 111.545 (**7a**) and 111.749 (**14b**) for hRXFP3 were thus obtained.

4.6.4. Sequence alignment

The sequences of hRXFP3 (Q8BGE9), hRXFP4 (Q8TDU9) and apelin receptor (5VBL) were downloaded from SWISS-MODEL (https://swissmodel.expasy.org/repository/uniprot/) and the alignment by CLUSTALW was performed on https://www.genome.jp/tools-bin/clustalw. The figure was plotted with ENDscript/ESPript 3.0 on http://espript.ibcp.fr/ESPript/cgi-bin/ESPript.cgi [19].

Declaration of Competing Interest

The authors declare that they have no known competing financial interests or personal relationships that could have appeared to influence the work reported in this paper.

Acknowledgements

We thank Sharon Layfield and Tania Ferraro for technical assistance. This work was partially supported by grants from the National Natural Science Foundation of China 81872915 (M.-W.W.), 82073904 (M-WW), 21302202 (QL) 81573479 (DHY) and 81773792 (DHY), the National Science & Technology Major Project “Key New Drug Creation and Manufacturing Program” of China (2018ZX09735-001 to M-WW, 2018ZX09711002-002-005 to DHY and 2018ZX09711002-002-011 to QL), the National Key R&D Program of China 2018YFA0507000 (M-WW) and Novo Nordisk-CAS Research Fund (NNCAS-2017-1-CC to DHY). The funders had no role in study design, data collection, and analysis, decision to publish, or manuscript preparation.

Author Contributions

QL, DHY and M-WW designed research. LL, GYL, QTZ, GQG and QL performed research, LL, GYL, QTZ, QL, RADB, DHY and M-WW analyzed data. LL, QL and M-WW wrote the manuscript.

Appendix A. Supplementary Data

Supplementary data for this article can be found online at XXX.

References and notes

[1] J. Grosse, H. Heffron, K. Burling, M.A. Hossain, A.M. Habib, G.J. Rogers, L. Parton, Insulin-like peptide 5 is an orexigenic gastrointestinal hormone, Proc. Natl. Acad. Sci. USA 111 (2014) 11133-11138, https://doi.org/10.1073/pnas.1411413111.

[2] M.L. Halls, R.A. Bathgate, S.W. Sutton, T.B. Dschietzig, R.J. Summers, International Union of Basic and Clinical Pharmacology XCV. Recent advances in the understanding of the pharmacology and biological roles of relaxin family peptide receptors 1-4, the receptors for relaxin family peptides, Pharmacol. Rev. 67 (2015) 389-440, https://doi.org/10.1124/pr.114.009472.

[3] R.A. Bathgate, M.L. Halls, E.T. van der Westhuizen, G.E. Callander, M. Kocan, R.J. Summers, Relaxin family peptides and their receptors, Physiol. Rev. 93 (2013) 405-480, https://doi.org/10.1152/physrev.00001.2012.

[4] R. Ivell, A.I. Agoulnik, R. Anand-Ivell, Relaxin-like peptides in male reproduction-a human perspective, Br. J. Pharmacol. 174 (2017) 990-1001, https://doi.org/ 10.1111/bph.13689.

[5] N.A. Patil, K.J. Rosengren, F. Separovic, J.D. Wade, R.A.D. Bathgate, M.A. Hossain, Relaxin family peptides: structure-activity relationship studies, Br. J. Pharmacol. 174 (2017) 950-961, https://doi.org/10.1111/bph.13684.

[6] M.A. Hossain, J.D. Wade, Synthetic relaxins, Curr. Opin. Chem. Biol. 22 (2014) 47-55, https://doi.org/10.1016/j.cbpa.2014.09.014.

[7] X. Luo, T. Li, Y. Zhu, Y. Dai, J. Zhao, Z.Y. Guo, M.W. Wang, The insulinotrophic effect of insulin-like peptide 5 in vitro and in vivo, Biochem. J. 466 (2015) 467-473, https://doi.org/ 10.1042/BJ20141113.

[8] S.Y. Ang, B.A. Evans, D.P. Poole, R. Bron, J.J. DiCello, R.A.D. Bathgate, M. Kocan, D.S. Hutchinson, R.J. Summers, INSL5 activates multiple signalling pathways and regulates GLP-1 secretion in NCI-H716 cells, J. Mol. Endocrinol. 60 (2018) 213-224, https://doi.org/10.1530/ JME-17-0152.

[9] D. Wei, M.J. Hu, X.X. Shao, J.H. Wang, W.H. Nie, Y.L. Liu, Z.G. Xu, Z.Y. Guo, Development of a selective agonist for relaxin family peptide receptor 3, Sci. Rep. 7 (2017) 3230, https://doi.org/10.1038/s41598-017-03465-7.

[10] S. Diwakarla, R.A.D. Bathgate, M.A. Hossain and J.B. Furness, Colokinetic effect of an insulin-like peptide 5 related agonist of the RXFP4 receptor, Neurogastroenterol. Motil. (2020) 32, e13796.

[11] S. Sudo, J. Kumagai, S. Nishi, S. Layfield, T. Ferraro, R.A. Bathgate, A.J. Hsueh, H3 relaxin is a specific ligand for LGR7 and activates the receptor by interacting with both the ectodomain and the exoloop 2, J. Biol. Chem. 278 (2003) 7855-7862, https://doi.org/10.1074/jbc.M212457200.

[12] S.Y. Ang, D.S. Hutchinson, N. Patil, B.A. Evans, R.A.D. Bathgate, M.L. Halls, M.A. Hossain, R.J. Summers, M. Kocan, Signal transduction pathways activated by insulin-like peptide 5 at the relaxin family peptide RXFP4 receptor, Br. J. Pharmacol. 174 (2017) 1077-1089, https://doi.org/10.1111/bph.13522.

[13] B. DeChristopher, S.H. Park, L. Vong, D. Bamford, H.H. Cho, R. Duvadie, O. Rozhitskaya, Discovery of a small molecule RXFP3/4 agonist that increases food intake in rats upon acute central administration, Bioorg. Med. Chem. Lett. 29 (2019) 991-994, https://doi.org/10.1016 /j.bmcl.2019.05.058.

[14] G.Y. Lin, L. Lin, X.Q. Cai, A.T. Dai, Y. Zhu, J. Li, Q. Liu, D.H. Yang, R. Bathgate, M.W. Wang, High-throughput screening campaign identifies a small molecule agonist of the relaxin family peptide receptor 4, Acta. Pharmacol. Sin. 41 (2020) 1328–1336, https://doi.org/10.1038/s41401-020-0390-x.

[15] K.A. Shaikh, S.R. Kande, C. B. Khillare, Boric acid catalyzed one-pot synthesis of [1,2,4] triazoloquinazolinone derivatives, IOSR J. Appl. Chem. 7 (2014) 54-58, https://doi.org/10.9790/5736-07515458.

[16] S.V. Ryabukhin, A. S. Plaskon, S.Y. Boron, D. M. Volochnyuk, A. A. Tolmachev, Aminoheterocycles as synthons for combinatorial Biginelli reactions, Mol. Divers. 15 (2011) 189-195, https://doi.org/10.1007/s11030-010-9253-6.

[17] A. V. Dolzhenko, A. V. Dolzhenkob, W. K. Chuia, Practical synthesis of regioisomeric 5(7)-amino-6,7(4,5)-dihydro[1,2,4]triazolo[1,5-a][1,3,5]triazines, Tetrahedron 63 (2007) 12888-12895, https://doi.org/10.1016/j.tet.2007.10.046.

[18] F. Shabanpoor, R. A. Hughes, R. A. D. Bathgate, S. Zhang, D. B. Scanlon, F. Lin, M. A. Hossain, F. Separovic, J. D. Wade, Solid-phase synthesis of europium-labeled human INSL3 as a novel probe for the study of ligand-receptor interactions, Bioconjug. Chem. 19 (2008) 1456-1463, https://doi.org/10.1021/bc800127p.

[19] X. Robert, P. Gouet, Deciphering key features in protein structures with the new ENDscript server, Nucleic Acids Res. 42 (2014) W320-W324, https://doi.org/ 10.1093/nar/gku316.

Highlights

A series of tricyclic derivatives were synthesized *via* Biginelli cyclocondensation.

The analogues were screened for their biological activities using a HTRF assay that measures the inhibition of forskolin-stimulated cAMP accumulation in human RXFP4-overexpressing CHO cells.

The specificity of the analogues for RXFP4 was also examined in human RXFP3-overexpressing CHO-K1 cells and human RXFP1-overexpressing 293T cells.

Compared with **7a**, compound 9-(*S*)-**14b** behaved as a RXFP4 agonist and exhibited 2.3-fold higher efficacy and better selectivity for RXFP4 *vs.* RXFP3.

A relatively high LibDock fitness score of 111.977 was obtained for the docking of **14b** with RXFP4, and several functions were involved including two hydrogen bonds, Pi-Pi stack and Pi-cation individually, and one additional Pi-sulfur function, which may explain the efficacy difference between **14b** and **7a**.